



Title	THERMAL STUDY OF GLASS TRANSITION AND DEVITRIFICATION PHENOMENA ON SOME SIMPLE MOLECULAR GLASSES
Author(s)	Sugisaki, Masayasu
Citation	大阪大学, 1968, 博士論文
Version Type	VoR
URL	<a href="https://hdl.handle.net/11094/308">https://hdl.handle.net/11094/308</a>
rights	
Note	

*The University of Osaka Institutional Knowledge Archive : OUKA*

<https://ir.library.osaka-u.ac.jp/>

The University of Osaka

DOCTORAL DISSERTATION

Title: THERMAL STUDY OF GLASS TRANSITION  
AND DEVITRIFICATION PHENOMENA ON  
SOME SIMPLE MOLECULAR GLASSES

Author: Masayasu Sugisaki

Work

performed at: Osaka University

Date: March 1968

## ABSTRACT

### THERMAL STUDY OF GLASS TRANSITION AND DEVITRIFICATION PHENOMENA ON SOME SIMPLE MOLECULAR GLASSES

by

Masayasu Sugisaki

In order to investigate thermodynamically the glass transition and the devitrification phenomena of some simple molecular glasses, we have constructed the two kinds of calorimeter. One of them is for such a purpose that the vitrification process is performed by a rapid cooling of a liquid sample in the calorimeter cell (Type-1), and the other is for the sample which is vitrified with condensation of its vapor directly on the chilled wall of the calorimeter cell (Type-2). The heat capacity measurements of isopentane, methanol and water were made for the crystalline, liquid, glassy and supercooled liquid states between 13° and 300°K. The details of the results are as follows.

(1) a) The heat capacity measurements were performed for the crystalline, liquid, glassy and supercooled liquid states of isopentane between 13° and 300°K by using the Type-1 calorimeter. b) The glass transition phenomenon of isopentane was found near 65°K with drastic change of the heat capacity which amounts to 68.20 J/mol°K).

c) The residual entropy of the glassy isopentane at absolute zero was found to be  $14.06 \text{ J}/(\text{mol}^\circ\text{K})$ . d) The irreversible entropy production of isopentane during the glass transition intervals was found to be  $0.08 \text{ J}/(\text{mol}^\circ\text{K})$ . It is concluded that the neglect of the irreversible production of entropy leads no significant error in determining the residual entropy.

(2) a) The heat capacity measurements of methanol were made for the crystalline state between  $20^\circ$  and  $120^\circ\text{K}$ , and for the glassy and supercooled liquid states between  $20^\circ$  and  $105^\circ\text{K}$  by using the Type-2 calorimeter. b) The glass transition phenomenon was found near  $103^\circ\text{K}$  with the abrupt change of the heat capacity which amounts to  $26 \text{ J}/(\text{mol}^\circ\text{K})$ . c) The drastic devitrification with the exothermic effect which amounts to  $1.54 \text{ KJ/mol}$  was observed near  $105^\circ\text{K}$ . The residual entropy for the glassy methanol at absolute zero was found to be  $7.07 \text{ J}/(\text{mol}^\circ\text{K})$ .

(3) a) In the case of water, the heat capacity measurements were carried out for the hexagonal crystal between  $60^\circ$  and  $250^\circ\text{K}$ , for the cubic crystal between  $20^\circ$  and  $240^\circ\text{K}$ , and for the glassy and supercooled liquid states between  $20^\circ$  and  $136^\circ\text{K}$  by using the Type-2 calorimeter. b) The glass transition phenomenon was found near  $135^\circ\text{K}$  with the sudden change of the heat capacity amounting  $35 \text{ J}/(\text{mol}^\circ\text{K})$ . c) The drastic devitrification

with the exothermic effect which amounts to 1.64 KJ/mol was observed at about 135°K. d) The transformation of the cubic crystal to the hexagonal one was found to occur irreversibly and sluggishly in the temperature region from 160° to 210°K where the exothermic effect coming to about 160 J/mol was observed.

Finally, the discussion is given concerning the origin of the glass transition phenomenon, and the definition of the glassy state.

It was concluded that the appearance of the glass transition phenomenon is due to the anomalous dispersion effect, although this phenomenon is closely connected with some thermodynamical quantities in the equilibrium state.

It was proposed that the non-crystalline solid deposited on the chilled substrate from the vapor state must show the glass transition phenomenon. This proposition was really confirmed by our experiments on methanol and water.

Definition of the glassy state was proposed in such a way that it must be in the thermodynamically non-equilibrium state, and that it must show necessarily the glass transition phenomenon.

THERMAL STUDY OF GLASS TRANSITION AND DEVITRIFICATION

PHENOMENA ON SOME SIMPLE MOLECULAR GLASSES

BY

MASAYASU SUGISAKI

1968

## ACKNOWLEDGMENT

The author would like to express his sincere thanks to Professor Syûzô Seki and Assistant Professor Hiroshi Suga of Osaka University, who have introduced him to this field of study, for valuable suggestions and advices throughout the course of this work, as well as for their assistances in refining the language and the scientific aspect of this paper.

The author is indebted to Messrs Keiichiro Adachi and Osamu Haida for their helps in part of the measurements, and to Miss Hiroko Nishikawa for typewriting a fair copy of this thesis.

## TABLE OF CONTENTS

	Page
[1] INTRODUCTION . . . . .	1
[2] EXPERIMENTAL . . . . .	7
2.1. Apparatus . . . . .	7
2.1.1. Type-1 Calorimeter. . . . .	7
2.1.2. Type-2 Calorimeter. . . . .	7
2.2. Sample . . . . .	17
2.2.1. Purification of the liquid samples. . .	17
2.2.2. Preparation of vitreous Samples . . .	18
[3] EXPERIMENTAL RESULTS . . . . .	22
3.1. Heat Treatment Adopted for the Heat Capacity Measurement . . . . .	22
3.1.1. Isopentane. . . . .	22
3.1.2. Methanol. . . . .	22
3.1.3. Water . . . . .	23
3.2. Results of Heat Capacity Measurement. . . .	25
3.2.1. Isopentane. . . . .	25
3.2.2. Methanol. . . . .	34
3.2.3. Water . . . . .	38
3.3. Thermodynamic Properties and Residual Entropy . . . . .	40
[4] DISCUSSION . . . . .	52
4.1. Glass Transition and Devitrification Phenomena . . . . .	52



	Page
4.1.1. Isopentane . . . . .	52
4.1.2. Methanol . . . . .	54
4.1.3. Water. . . . .	55
4.2. Origin of Glass Transition Phenomenon. . . .	67
4.3. Appearance of Glass Transition Phenomenon as a Temperature Dispersion . . .	72
4.4. Entropy Production and Residual Entropy . . . . .	79
4.5. Definition of Glassy State . . . . .	81
[5] CONCLUSION. . . . .	84
[6] BIBLIOGRAPHY. . . . .	87

# LIST OF TABLES

	Page
1. Summary of Previous Experimental Data . . . . .	6
2. Experimental Data of Methanol . . . . .	20
3. Experimental Data of Water. . . . .	21
4. Heat Capacity of Isopentane	
(A) crystal and liquid. . . . .	26
(B) glass and supercooled liquid. . . . .	27
5. Heat of Fusion of Isopentane. . . . .	29
6. Heat Capacity of Methanol	
(A) crystal . . . . .	36
(B) glass and supercooled liquid. . . . .	36
7. Heat Capacity of Water	
(A) hexagonal ice . . . . .	43
(B) glass and supercooled liquid. . . . .	44
(C) cubic ice . . . . .	45
8. Total Amount of Exothermic Effect Accompanying Irreversible Transformation of Cubic to Hexagonal Ice . . . . .	48
9. Thermodynamic Properties of Isopentane	
(A) crystalline and liquid states . . . . .	49
(B) glassy and supercooled liquid states. . . . .	50
10. Thermodynamic Properties of Methanol (glassy and supercooled liquid states) . . . . .	51
11. Comparison of Previous Data for Heat of Devitrification . . . . .	62

## LIST OF FIGURES

	Page
1. Description of the Type-1 Calorimeter . . . . .	8
2. Description of the Type-2 Calorimeter . . . . .	12
3. Description of the Sample Container . . . . .	13
4. Heat Capacity Curve of Isopentane . . . . .	28
5. Melting Curve of Isopentane . . . . .	30
6. Heat Capacity Curve of Isopentane in the Region of the Glass Transition Temperature . . . . .	32
7. Enthalpy Curve of Isopentane near the Glass Transition Point. . . . .	33
8. Heat Capacity Curve of Methanol . . . . .	37
9. Heat Capacity Curve of Water. . . . .	41
10. Heat Capacity Curve of Water near the Glass Transition Temperature. . . . .	42
11. Heat Capacity of Ice. . . . .	46
12. Heat Capacity of Ice near the Transformation Temperature. . . . .	47
13. Heat Capacity of the Glassy State of Water. . . . .	57
14. Enthalpy Relationship of Various States of Water. . . . .	59
15. (A) Units of Conformation of Oxygen Atoms . . . . .	65
15. (B) Models of the Crystal Structure of Ice. . . . .	66
16. Entropy Curve of Isopentane . . . . .	69
17. Temperature Dependence of the Relaxation Time . . . . .	74
18. Sketch of the Typification of the Hypothetical Heat Flow in a Liquid . . . . .	77

## [1] INTRODUCTION

When liquid materials are supercooled down far below their melting points without any crystallization effect, a certain kinds of their physical properties, such as heat capacity, thermal expansion, and compressibility as static properties, as well as dynamical properties such as viscosity and others, are observed to change abruptly at a narrow temperature region characteristic of each material. This characteristic temperature, which is called now as a glass transition temperature  $T_g$ , was first observed by Regnault<sup>(1)</sup> in 1856 on selenium element. The importance of this discovery has been, however, overlooked for about 70 years, the modern investigation on this phenomenon was restarted by the celebrated work by Simon<sup>(2)</sup> on glucose in 1922. Since then there have been increasing such kind of investigations intermittently. The development of the synthetic high polymer chemistry has accelerated the more detailed study on this field and now we have a considerable number of data about the glass transition on various kind of materials.

Now, below this boundary of temperature, so-called glass transition temperature  $T_g$ , the supercooled liquid

transforms into a new state which is called as a glass. This glassy state is definitely distinguished from the supercooled liquid by only the fact that its internal equilibrium is not attained. A glass is often called also as a non-crystalline or amorphous solid, because the glass lacks a long-range periodicity characteristic of a crystalline state, and that, responds against an external force likely as a solid.

Nowadays, we are able to obtain the non-crystalline solids by using other various methods<sup>(3)</sup> except the method of the supercooling of liquid. These methods are, shock wave treatment, neutron bombardment, vapor condensation, solution method (hydrolysis and anodization methods), and finally dehydration of hydrated crystal. These non-crystalline solids prepared by the different methods have common features that they crystallize below their melting point on heating. Are they plausible to be also called as a glass? In order to reply this question, it seems most decisive to find out their glass transition phenomena. Up to the present time there has been no successful and quantitative work of observing the glass transition phenomena for such non-crystalline solids. In addition to the above-mentioned question, there is very important unsolved problem concerning the essential nature of the glass transition

phenomenon. About this problem there exist two kinds of opposite opinion. One is such that the glass transition occurs at temperature where a certain kind of thermodynamical quantity takes critical value<sup>(4,5)</sup>. The other is such that the glass transition phenomenon may be interpreted as a relaxation phenomenon with regards to the degree of freedom of molecular motions. In order to resolve this controversy, it seems very appropriate to perform the accurate experiments about the glasses composed of as simpler molecule as possible, and analyze the results from thermodynamical and dynamical aspects.

For these purposes of resolving the two important problems, we constructed two types of calorimeter and performed the heat capacity measurement for vitreous isopentane, methanol and water using the supercooling and the vapor condensation methods. Before proceeding to the description of the details of our original work we should like to present below some available knowledge on each materials reported by previous workers for references.

a) For isopentane there is known that the binary mixtures of this compound with some hydrocarbons (e.g. 3-methylpentane) are easily supercooled and often used as a matrix for isolation technique of free radicals

or excited molecules, but pure isopentane is supercooled with some difficulty, and that, its glass transition phenomenon has not yet been observed before the present study.

b) The glassy states of the many alcohols are well known except methanol as the simplest alcohol. According to Staveley et al.<sup>(6)</sup> pure methanol can be supercooled down to 95°K when its droplet is chilled down. Pimentel<sup>(7)</sup> has also reported that the infrared absorption spectra of methanol deposited on the cold substrate at about 4°K is considered as that for its glassy state. In spite of these observations it has not been yet clarified whether these two uncommon states are really called as a glass.

c) Finally, concerning water there exists no successful work of obtaining a glassy state by a rapid cooling of liquid water at the present time. However, it has been well known that the binary systems such as  $\text{H}_2\text{O}-\text{N}_2\text{H}_4$ <sup>(8)</sup>,  $\text{H}_2\text{O}-\text{HCl}$ <sup>(9)</sup>, and  $\text{H}_2\text{O}-\text{Ca}(\text{NO}_3)_2$ <sup>(10)</sup> become easily glassy state by rapid cooling of solutions. In these cases, their glass transition points have been found between 140° and 150°K.

On the other hand, many previous workers have reported that even a pure water becomes non-crystalline solid when the vapor is condensed directly on a suf-

ficiently chilled substrate. Recently, McMillan and Los<sup>(11)</sup> have reported that they have found a glass transition point of the condensed non-crystalline solid of water at 139°K using the differential thermal analysis method. Furthermore, many previous workers have reported by use of the X-ray or electron diffraction methods that the amorphous ice crystallizes into a cubic form when heated up to 140°K, and that cubic ice transforms into a hexagonal ice sluggishly and irreversibly on heating up to about 200°K. All the informations hitherto obtained by many workers with different methods of investigation on the relationship among the non-crystalline solid, the hexagonal ice and the cubic ice, are summerized in Table 1.



Table 1. Summary of Previous Experimental Data.

Experimental Method	Temperature Region (°C)							Number of Bibliography		
	-180	-160	-140	-120	-100	-80	-60			
								Worker		
X-ray diffraction	amorphous			semi-crystalline		hexagonal		Burton & Oliver (1935)	12	
thermal analysis	amorphous			crystalline				Staronka (1939)	13	
X-ray diffraction	+ small crystals	intermediate range not investigated				+ hexagonal		Vegard & Hillesund (1942)	14	
electron diffraction	small crystals	cubic				hexagonal		König (1942)	15	
thermal analysis	amorphous			crystalline				Pryde & Jones (1952)	16	
electron diffraction	crystal growth poor	cubic				hexagonal		Honjo et al. (1956)	17	
thermal analysis	amorphous			crystalline				Ghormley (1956)	18	
thermal analysis	amorphous			crystalline				de Nordwall & Staveley (1956)	19	
electron diffraction	amorphous or small crystals			cubic	hexagonal			Blackman & Linsgarten (1957)	20	
X-ray diffraction	amorphous			cubic	hexagonal				Shallcross & Carpenter (1957)	21
X-ray diffraction	amorphous	cubic	hexagonal					Dowell & Rinfret (1960)	22	
electron diffraction	halo pattern	cubic	hexagonal					Shimaoka (1960)	23	
X-ray diffraction	amorphous			cubic			hexagonal	Beaumont et al. (1961)	24	
differential thermal analysis	glass			cubic	hexagonal			McMillan & Los (1965)	11	
supercooled liquid?										

## [2] EXPERIMENTAL

### 2.1. Apparatus

In the present work, we have constructed the two kinds of calorimeter. One of them is for such a purpose that the vitrification process is performed by a rapid cooling of a liquid sample in the calorimeter cell, and the other is for the sample which is vitrified with condensation of its vapor directly on the chilled wall of the calorimeter cell.

2.1.1. Type-1 Calorimeter. The adiabatic Nernst-type calorimeter used hitherto in our laboratory<sup>(25)</sup> was partly modified, in such a way that a rapid quenching of the liquid sample may be easily carried out. For this purpose, an additional transfer tubing made of stainless-steel is provided which enables charging of liquid nitrogen or liquid hydrogen directly into the space between the outer and the inner adiabatic shields as is shown in Fig. 1.

2.1.2. Type-2 Calorimeter. In the past, there has been known no successful work of the precise

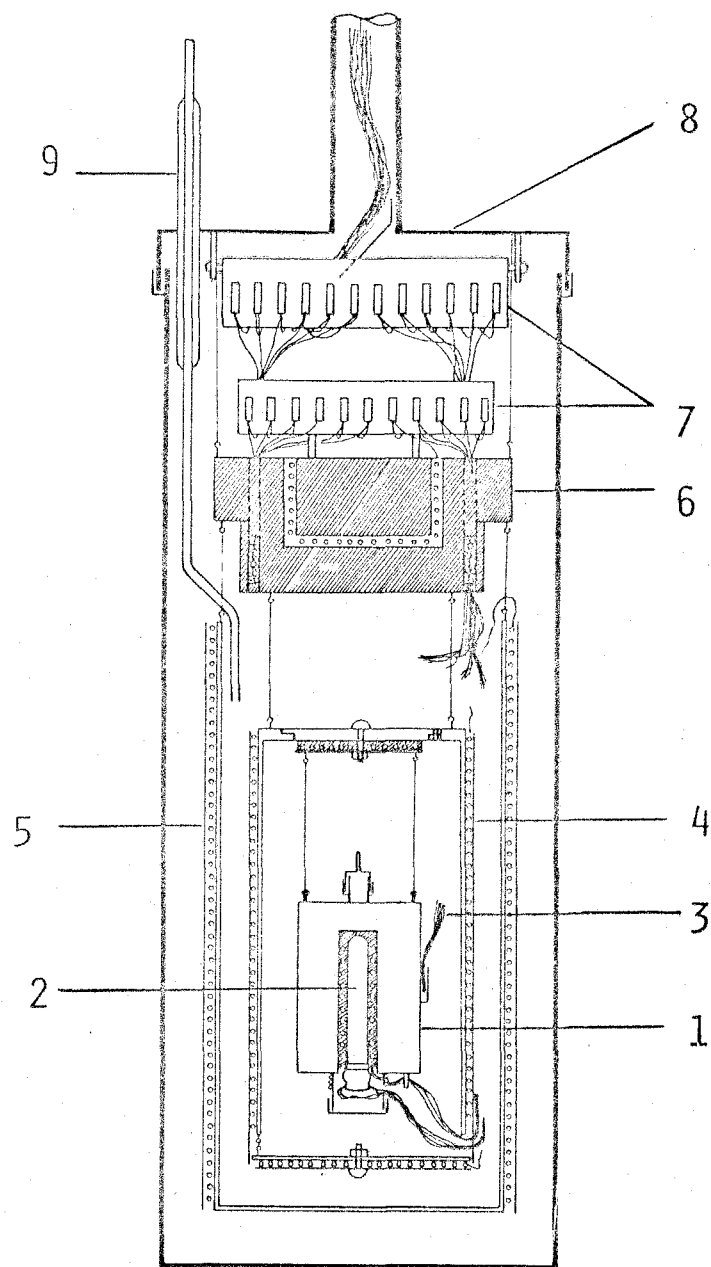


Fig. 1. Description of the Type-1 Calorimeter.

- 1) sample container, 2) platinum resistance thermometer, 3) thermocouple, 4) inner shield, 5) outer shield, 6) copper block, 7) lead connector, 8) vacuum jacket, 9) transfer tube.

measurement of heat capacities for an amorphous material deposited directly onto the wall of a calorimeter cell from its vapor state. This fact is due to some difficulties for constructing the calorimeter which fulfills the following rather severe requirements.

(a) The calorimeter must be equipped with the filling tube, through which vapor of a sample passes, kept at a sufficiently higher temperature above the melting point of the sample, and with the calorimeter cell into which the vapor of the sample is condensed as an amorphous state, kept at a sufficiently lower temperature far below a glass transition temperature of the amorphous sample. For instance, the temperature of the filling tube should be higher about  $100^{\circ} \sim 200^{\circ}\text{C}$  than that of the calorimeter cell if the glass transition point of the sample used situates around  $100^{\circ}\text{K}$ .

(b) In order to satisfy the above cited steady distribution of temperature difference in the calorimeter, a thermal switch is required whose power of heat exchange is sufficiently large enough.

(c) It seems very difficult to obtain a considerable amount of a condensed amorphous substance, so a good adiabatic conditioning of the calorimeter is needed in order to perform precise measurements.

In order to satisfy the condition (a), all previous workers have adopted the method that a sample cell is directly immersed into the liquid nitrogen. This method is, however, inadequate to satisfy the condition (c), because a contamination during the sampling obstructs a realization of an adiabatic conditioning by high vacuum. By taking into consideration the above cited three conditions we have constructed the calorimeter with adopting following devices.

(a) In order to maintain the steady temperature difference between the sample cell and the filling tube, the heat conduction between them is sufficiently reduced by joining them through a thin stainless tube (3 mm in diameter, 0.15 mm in thickness and 10 mm in length). (b) For simplicity of the handling of the apparatus, a conduction gas method was chosen as the thermal switch. If we adopt a mechanical thermal switch which has a comparable efficiency of heat exchange with that of the conduction gas thermal switch, the apparatus becomes to be very complicated. This complication necessarily causes the increase of heat capacity of the sample cell itself, so the mechanical switch is inadequate for the precise measurement. (c) In order to realize a good adiabatic condition, it seems

preferable to design the calorimeter equipped with two adiabatic jackets; the structure satisfies the conditions that the convection current of the conduction gas is facilitated, and that a heat leak due to a radiation is completely precluded.

Based on these considerations mentioned above, we have constructed a calorimeter which consists of a filling tube made of monel and soft copper, a copper cell with a platinum resistance thermometer, inner and outer adiabatic jackets, a copper block as thermal station, and a vacuum jacket and others. This filling tube, two adiabatic shields and a copper block are all wound closely with constantan heaters.

The total view of the constructed calorimeter and the sketch of the sample cell are given in Figs. 2 and 3. As is shown in the Fig. 3, the part of the filling tube enters into the sample cell. During the procedure of sampling, this part of the filling tube is warmed by the heat conduction from the upper part of the filling tube which is wound closely with the constantan heater. The part of the filling tube inside the cell can be kept at about 15°C, when the temperature of the wall of the sample cell is adjusted to be about 80°K and the outer part of the filling tube is warmed around

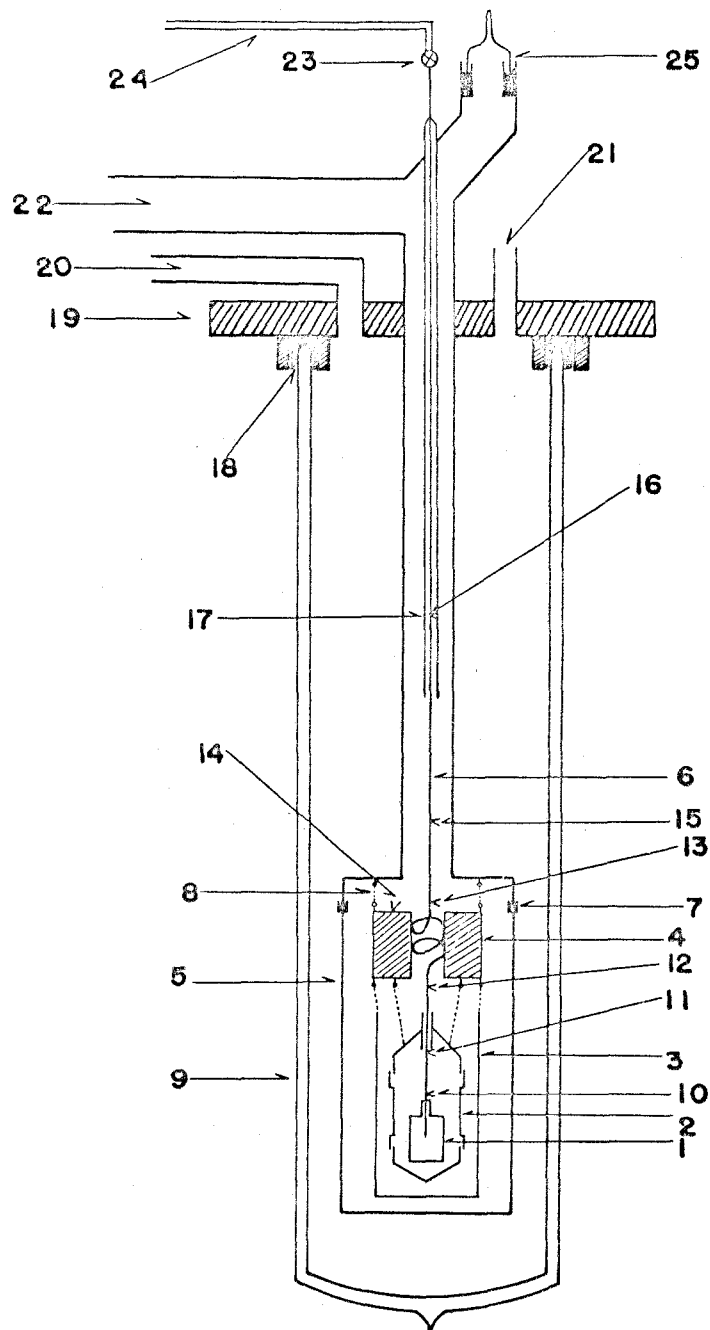


Fig. 2. Description of the Type-2 Calorimeter.

1) sample container, 2) inner shield, 3) outer shield, 4) copper block. 5) vacuum jacket, 6) filling tube, 7) wood alloy joint, 8) nylon thread, 9) glass dewar, 10) ~ 16) thermocouples, 17) sheath of the filling tube, 18) picein joint, 19) brass plate for supporting the apparatus, 20) outlet tube, 21) tube for introducing liquid hydrogen or nitrogen, 22) to vacuum pumps, 23) needle valve for sampling, 24) glass tube for introducing the vapor of sample, 25) picein joint for taking out of lead wires.

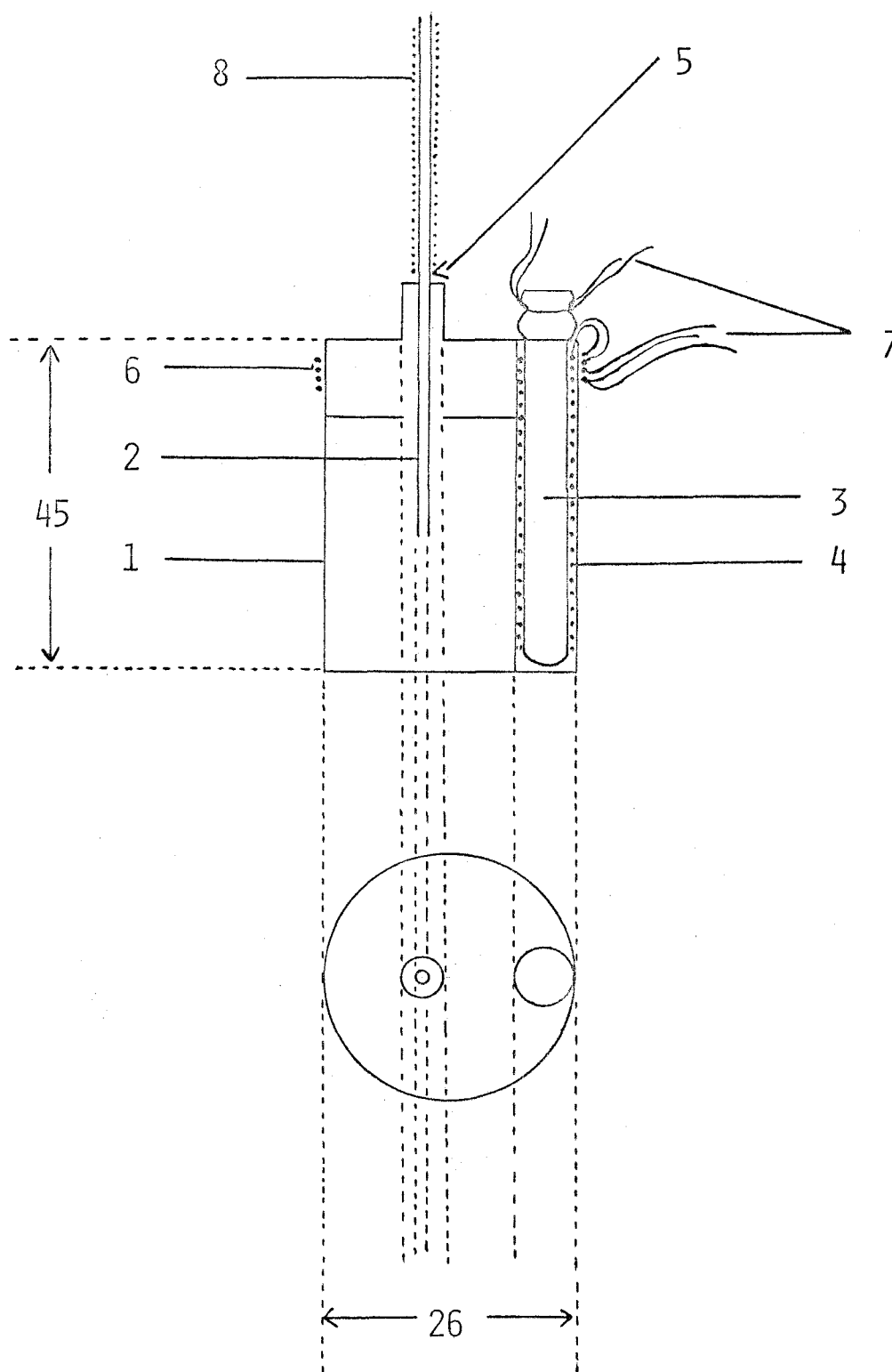


Fig. 3. Description of the Sample Container.

- 1) wall of the cell (made of copper),
- 2) filling tube, 3) platinum resistance thermometer,
- 4) constantan heater for energy-input, 5) thermocouple,
- 6) and 7) lead wires, 8) heater for sampling.



30°C under high vacuum condition of about  $10^{-6}$  mm Hg inside the cell. In this case the heat conduction between the filling tube and the sample cell occurs spontaneously through the outer short stainless steel tubing put on the top of the cell. The amount of this heat conduction is estimated as 1.3 (J/s), when the above cited temperature difference is adjusted. Therefore the effect of the thermal switch is necessitated whose power of the heat exchange is at least larger than 1.3 (J/s). For this purpose the conduction gas method by using helium gas is sufficiently adequate when the apparatus is operated above the boiling point of liquid nitrogen.

In order to carry out the heat capacity measurement under well adiabatic condition, the adequate combination of monel and copper metals for the filling tube outside the cell is designed for preventing the heat leak through this tube.

Measurements of temperature are made with the platinum resistance thermometer calibrated in terms of International Temperature Scale between 90°K and 500°K and the provisional scale of the National Bureau of Standards between 11°K and 90°K.

It is found that a heat capacity of the empty cell

is about 8.5 (J/degK) at room temperature, and that the attainment of the thermal equilibrium after the finish of energy input takes about 25 minutes at all temperature region between 13° and 330°K, and that the values of heat capacity deviates from the smoothed curve within 0.1 % in the temperature region between 13° and 330°K.

Next, the procedures for condensing the vapor of a sample into the calorimeter as an amorphous state will be described. Firstly the vacuum jacket is immersed into the liquid nitrogen, and helium gas at about one atmospheric pressure is then introduced as a conduction gas into the vacuum jacket, the filling tube and the copper block being simultaneously warmed up at the desired temperature with the constantan heaters wound around them. Their temperatures are registered by the seven chromel P-constantan thermocouples, one of which is attached on the copper block, all the others being attached on the filling tube (see Fig. 2). The temperature of the sample cell is watched by recording the resistance of the platinum thermometer on the "Speedo Max" (Type G, Leeds & Northrup Co.). Under such operation of the heaters, only the wall of the sample cell is chilled down to sufficiently low temperature, because the heat exchange between the

filling tube and the sample cell is pressed down. The temperature difference between them can be easily regulated at any desired values up to about 200°C by changing the level height of liquid nitrogen or by changing the amount of electric current through the heater wound on the filling tube. When the temperature distribution of the calorimeter becomes to be steady, the vapor of the sample is slowly condensed into the calorimeter by opening the needle valve situated at the upper part of the calorimeter (see Fig. 2). The rate of condensation must be regulated to be very slow, since the surface of the amorphous sample produced in the cell may be warmed up above a devitrification temperature with the accumulation of the heat of condensation if the rate of condensation is pretty high. Usually the preparation of the vitreous sample needs about 10 ~ 20 hours and a total amount of a condensed vitreous substance is of about 1 ~ 2 g. After the sampling is over, the heaters of the filling tube and of the copper block are switched off, and the total parts of the calorimeter are chilled down to 80°K, then helium gas (20 mmHg at 80°K) being introduced in the calorimeter cell in order to facilitate the attainment of the thermal equilibrium. Finally the conduction gas in the vacuum jacket is evacuated

down to  $10^{-6}$  mm Hg for the maintenance of the adiabatic condition. Measurements of the heat capacities were carried out from 13°K to 330°K.

When the measurement is over, the calorimeter cell is heated up and the sample in the cell is gathered in the glass tube out of the calorimeter, and its total amount is determined by measuring its weight.

## 2.2. Sample

2.2.1. Purification of the liquid samples. (a) Isopentane. The commercial extra pure isopentane (Nakarai Chemicals, Ltd.) was purified by fractional distillation, and then distilled twice under high vacuum ( $10^{-6}$  mm Hg). Impurities contained in each fraction were detected by use of the gas-chromatographic technique and the purest fraction was employed for the heat capacity measurements. The amount of the impurities present in the sample was determined to be 0.014 mole percent by making use of thermo-analytical method as will be described later.

(b) Methanol. The commercial extra pure methanol (Wako Chemical Industries, Ltd.) was dried by magnesium metal (Lund and Bjerrum method). This product was

distilled twice in high vacuum ( $10^{-6}$  mm Hg) and the final product was degassed very carefully by repeating melting and freezing of the sample under high vacuum ( $10^{-6}$  mm Hg). This final product was introduced in the calorimeter in high vacuum ( $10^{-6}$  mm Hg).

(c) Water. The water treated by ion-exchange resin was distilled under atmospheric pressure, and then this product was distilled twice in high vacuum ( $10^{-6}$  mm Hg). After the final product was degassed very carefully with the same procedure mentioned above, the sample was condensed into the calorimeter in high vacuum ( $10^{-6}$  mm Hg).

2.2.2. Preparation of vitreous samples. (a) Isopentane. In this case, the Type-1 calorimeter was used. The liquid sample (0.2433 mol) sealed under high vacuum in a gold calorimeter cell, was quenched down to 20°K from room temperature by use of liquid hydrogen. It was found that the whole amount of the sample was completely supercooled down to 20°K without any occurrence of crystallization.

(b) Methanol. For this material the Type-2 calorimeter was employed, and the outer jacket was removed so that the temperature of the sample cell

may be kept as low as possible. During the vitrification process, the temperature of the sample cell was kept between  $94^{\circ}$  and  $97^{\circ}\text{K}$ , and the filling tube around  $220^{\circ}\text{K}$ . The two kinds of rate of condensation were adopted as given in Table 2.

(c) Water. In this case the Type-2 calorimeter equipped with the outer jacket was used so that measurements of the heat capacity in high temperature region can be easily performed. During the vitrification, the temperature of the sample cell was kept between  $103^{\circ}$  and  $106^{\circ}\text{K}$  for sample (1), and between  $120^{\circ}$  and  $123^{\circ}\text{K}$  in the other cases of samples (2), (3) and (4). The filling tube was kept around  $300^{\circ}\text{K}$  in each case for all samples. The rate of condensation and the total amount of the sample used for the measurements are given in Table 3.

Table 2. Experimental Data of Methanol.

Number of sample	Rate of condensation (g/hr.)	Total amount of sample (g)	Heat of devitrification (KJ/mol)	$\Delta C_p$ at $T_g$ (J/mol $^\circ$ K)	Amorphous part of sample (%)	
1	0.101	1.214	1.54	} $\pm 0.05$	26	100
2	0.366	1.645	0.57		10	37.4

Table 3. Experimental Data of Water.

Number of sample	Rate of condensation (g/hr.)	Total amount of sample (g)	Heat of devitrification (KJ/mol)	$\Delta C_p$ at $T_g$ (J/mol $^\circ$ K)	Amorphous part of sample (%)	
1	0.032	0.6054	1.64	} $\pm 0.05$	35	100
2*	0.033	0.5897	1.46		29	89.0
3**	0.024	0.6959	1.06		19	64.6
4***	0.030	0.7745	0.85		11	49.0

\*: annealed at 128 $^\circ$ K for 4 hours.

\*\*: annealed at 128 $^\circ$ K for 16 hours.

\*\*\*: annealed at 128 $^\circ$ K for 13 hours.



### [3] EXPERIMENTAL RESULTS

#### 3.1. Heat Treatment Adopted for the Heat Capacity Measurement.

3.1.1. Isopentane. The measurements of heat capacities of the crystalline and liquid states were made from 13° to 300°K. The measurements for the glass were made from 15°K to just above the glass transition temperature. In the glass transition intervals detailed measurements were also made for various samples which had experienced the different thermal histories. After the measurements of the quenched sample were made from 15° to 68°K, the sample was slowly cooled down to 43°K during 4 hours. The measurements for this sample were made from 43° to 68°K. Finally, this sample was again chilled down to 60°K from 68°K during 25 minutes and annealed for about 20 hours at this temperature. The measurements for this annealed sample were also made from 60° to 68°K.

3.1.2. Methanol. For the sample (1) heat capacities

of glassy state were measured from 94°K to just above the glass transition temperature, and this sample was again chilled down slowly to 80°K as soon as the sample reached to just above the glass transition temperature, and heat capacities were measured again from 80° to 104°K. When the temperature of the sample reached about 105°K, a drastic devitrification took place and the temperature of the sample rises spontaneously due to the exothermic effect. For the sample (2) the measurements were made for the glassy state from 20° to 104°K. After the devitrification, the crystalline sample was chilled down to 20°K and the measurements were made from 20° to 120°K.

3.1.3. Water. Sample (1). The measurements of heat capacities of a glassy state were made in the region covering the glass transition temperature, when an appreciable exothermic effect was observed above 115°K. The drastic devitrification was observed at about 135°K which is just above the glass transition point.

Sample (2). The measurements for the glassy state were made in the region of glass transition temperature, when the exothermic effect was observed above 123°K.

The drastic devitrification was observed at about 135°K. After the devitrification is over this sample was chilled down to 110°K and measurements were carried out from 180° to 237°K, when the appreciable exothermic effect was observed between 180° and 210°K. After the previous series of measurement, this sample was chilled down to 180°K and the measurements were made from 180°K to 225°K.

Sample (3). Prior to the measurement of the glassy state, the sample was annealed at 128°K for 12 hours. The measurements of the glassy state were made from 20° to 135°K. After the devitrification is performed, this sample was chilled down to 20°K, and the measurements were made again from 20° to 240°K, an appreciable exothermic effect being also observed between 160° and 210°K during this experiment. This sample was again chilled down to 60°K and the measurements were carried out from 60° to 240°K.

Sample (4). After the measurement of the glassy state between 60° and 125°K was over, the sample was annealed at 128°K for 12 hours, and then for this annealed sample the measurements were made between 120° and 135°K, when the drastic devitrification was observed at about 135°K. After the completion of this

devitrification, the sample was chilled down to 60°K and the measurements were repeated from 60° to 240°K.

### 3.2. Results of Heat Capacity Measurement.

3.2.1. Isopentane. (a) Heat capacities of its crystalline and liquid states. The numerical values are given in Table 4A and illustrated by hollow circles in Fig. 4. These values agree with those reported by Guthrie and Huffman<sup>(26)</sup> in 1943 with the experimental error. They confirmed the non-existence of the appearance of anomalous heat capacity of the liquid state in the temperature region between 170° and 250°K which was first reported by Schumann and Aston<sup>(27)</sup> in 1942. This fact coincides with our present results.

The data of melting point in relation to the mole fraction of the melt, and the heat of fusion, obtained from the results of heat capacity measurements, are shown in Table 5, and the relationship between the melting points and the reciprocal molten fraction is given in Fig. 5. The value obtained for the melting point of 100 % pure isopentane is found to be  $113.36 \pm 0.05^\circ\text{K}$ . From the melting curve, the

Table 4A. Heat Capacity of Isopentane  
(crystal and liquid) in J/(mol°K).

T(°K)	Cs	T(°K)	Cs	T(°K)	Cs
series 1		85.90	68.121	168.44	132.24
14.99	6.414	87.86	69.683	170.58	132.58
16.87	8.624	89.78	71.167	172.73	133.05
18.61	10.848	91.67	72.520	174.86	133.52
20.40	12.928	93.53	73.888	177.00	133.88
22.51	15.736	95.37	75.232	179.12	134.28
24.49	18.259	97.18	76.654	181.24	134.63
26.40	20.447	98.96	77.920	183.36	134.92
28.34	22.632			185.47	135.31
30.31	25.200	series 3			
32.67	27.777	97.20	75.764	series 6	
35.12	30.402	98.95	78.217	165.68	131.76
37.37	32.686	100.68	79.152	168.23	132.24
39.68	34.908	102.40	80.558	171.13	132.68
42.07	36.936	104.11	81.997	173.88	133.13
44.42	38.989	105.77	83.456	176.62	133.69
46.88	41.136	107.40	84.532	179.35	134.27
49.31	43.106	109.02	85.962	182.07	134.76
51.64	44.892	110.61	88.151	184.78	135.25
53.86	46.681	112.13	96.408	187.49	135.73
56.09	48.520	113.36	123.38	190.18	136.21
58.32	50.428	114.83	124.83	192.87	136.76
60.48	52.357			195.54	137.28
62.57	54.188	series 4		198.21	137.83
64.16	55.726	119.70	124.51	200.87	138.36
66.15	57.753	121.53	124.63	203.52	138.99
68.12	60.251	123.36	124.92	206.16	139.38
70.10	63.005	125.19	125.05	208.79	140.08
72.04	62.502	127.23	125.52	211.41	140.56
74.00	60.598	129.50	125.62	214.02	141.13
75.95	61.336	131.76	125.99	216.63	141.81
77.86	62.457	134.01	126.42	219.22	142.33
79.74	63.896	136.25	127.02	221.81	142.91
		138.49	127.66	226.66	144.24
series 2		140.72	127.89	229.22	144.74
60.18	51.999	142.94	128.34	231.76	145.56
62.43	54.179	145.15	128.74	234.30	146.13
64.60	56.669	147.36	129.00	236.83	146.74
66.69	58.302	149.56	129.23	239.47	147.22
68.72	60.140	151.77	129.76		
70.69	63.533			series 7	
72.61	62.931	series 5		234.70	145.95
74.54	60.829	155.44	130.38	237.12	146.76
76.46	61.513	157.62	130.64	239.52	147.65
78.35	62.634	159.79	130.80	241.91	148.30
80.20	64.840	161.96	131.21	244.29	148.78
82.01	65.343	164.13	131.31	246.65	149.49
83.91	66.851	165.68	131.76	(to be continued)	

Table 4A. (Continued)

T (°K)	Cs	T (°K)	Cs	T (°K)	Cs
249.01	150.11	265.28	154.96	281.68	160.16
251.36	150.88	267.57	155.65	284.50	161.05
253.72	151.64	269.84	156.59	287.30	161.92
256.07	152.41	272.10	157.25	290.08	162.98
258.39	153.12	274.36	157.95	292.85	164.17
260.69	153.83	276.46	158.56	295.61	165.15
262.99	154.60	278.85	159.13	298.34	166.17

Table 4B. Heat Capacity of Isopentane

(glass and supercooled liquid) in J/(mol°K).

T (°K)	Cs	T (°K)	Cs	T (°K)	Cs
Glass		60.61	61.971	62.77	65.565
		62.71	65.400	63.70	72.107
series 1		64.92	75.800	64.98	82.561
15.60	9.398	66.54	116.04	65.37	96.907
17.34	11.707	67.66	117.79	Supercooled liquid	
19.06	13.834	68.62	117.87		
20.61	15.779				
22.59	18.289	series 2		66.02	116.34
24.47	20.546	45.88	41.615	66.69	117.47
26.28	22.764	48.30	43.630	67.35	117.62
28.14	24.850	54.60	45.630	68.31	117.79
30.05	26.976	52.79	47.810	69.59	117.78
32.34	29.462	54.90	50.016	70.85	117.60
34.73	31.882	56.92	52.436	72.12	118.07
36.93	34.042	58.99	55.676	73.39	117.78
38.99	35.852	61.08	60.210	74.67	118.13
41.03	37.612	63.09	67.832	series 4	
43.08	39.302	64.82	90.959		
45.33	41.103	66.20	117.61	105.96	122.38
47.78	43.325	67.30	117.66	107.45	122.49
50.33	45.659	68.24	117.68	108.93	122.71
52.54	47.773	series 3		110.41	122.97
54.67	50.115			111.89	123.03
56.72	52.939	60.79	57.671		
58.79	56.253	61.75	60.944		

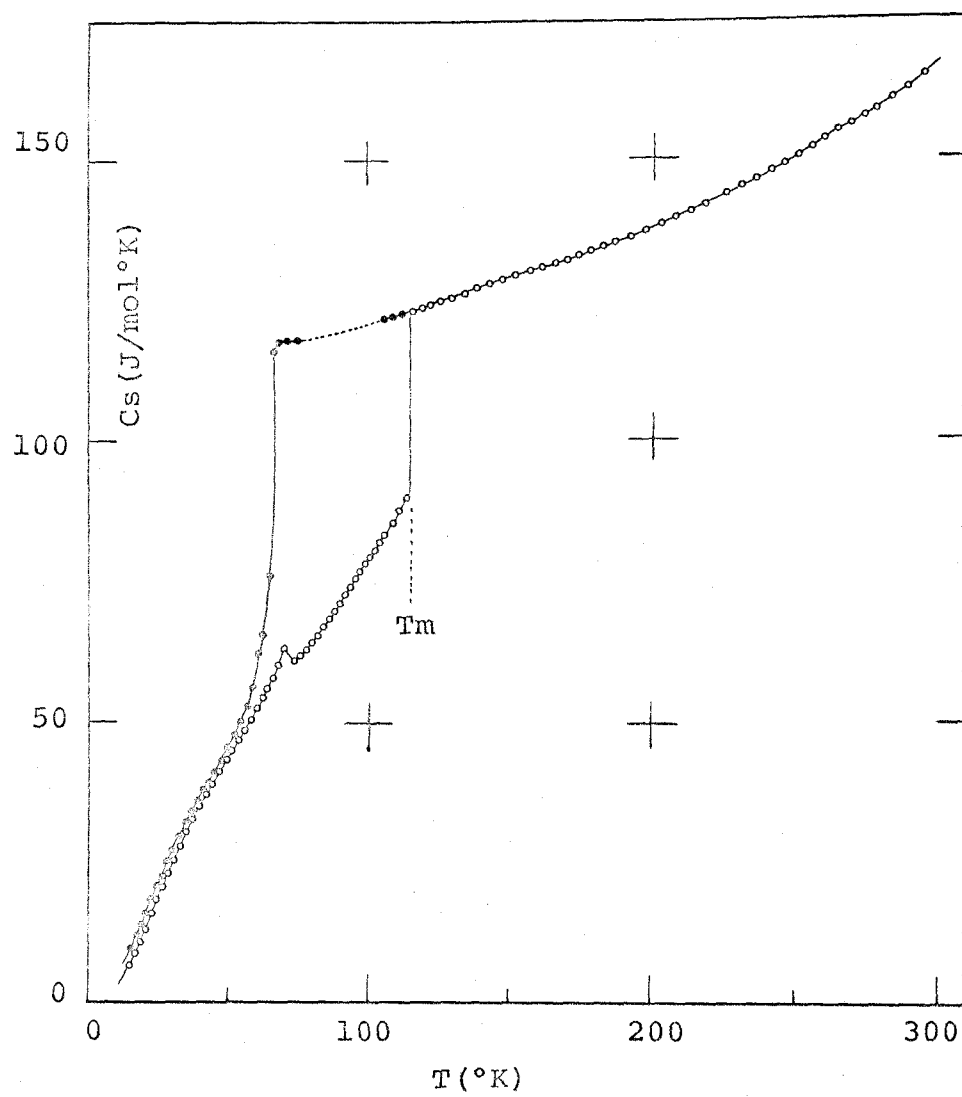


Fig. 4. Heat Capacity Curve of Isopentane.

Table 5. Heat of Fusion of Isopentane.

T(°K)	$\int \Delta C_p dT$	1/r
Melting point	Heat input (J/mol)	Reciprocal molten fraction
113.341	601.9	8.73
.347	820.7	6.19
.348	1039.8	4.88
.351	1258.7	4.03
.352	1477.7	3.44
.353	1759.3	2.89
.355	2041.0	2.49
.356	2322.5	2.19
.357	2885.5	1.76
.357	3448.1	1.47
.358	4339.7	1.17

( Heat of fusion: 5140±2 J/mol)



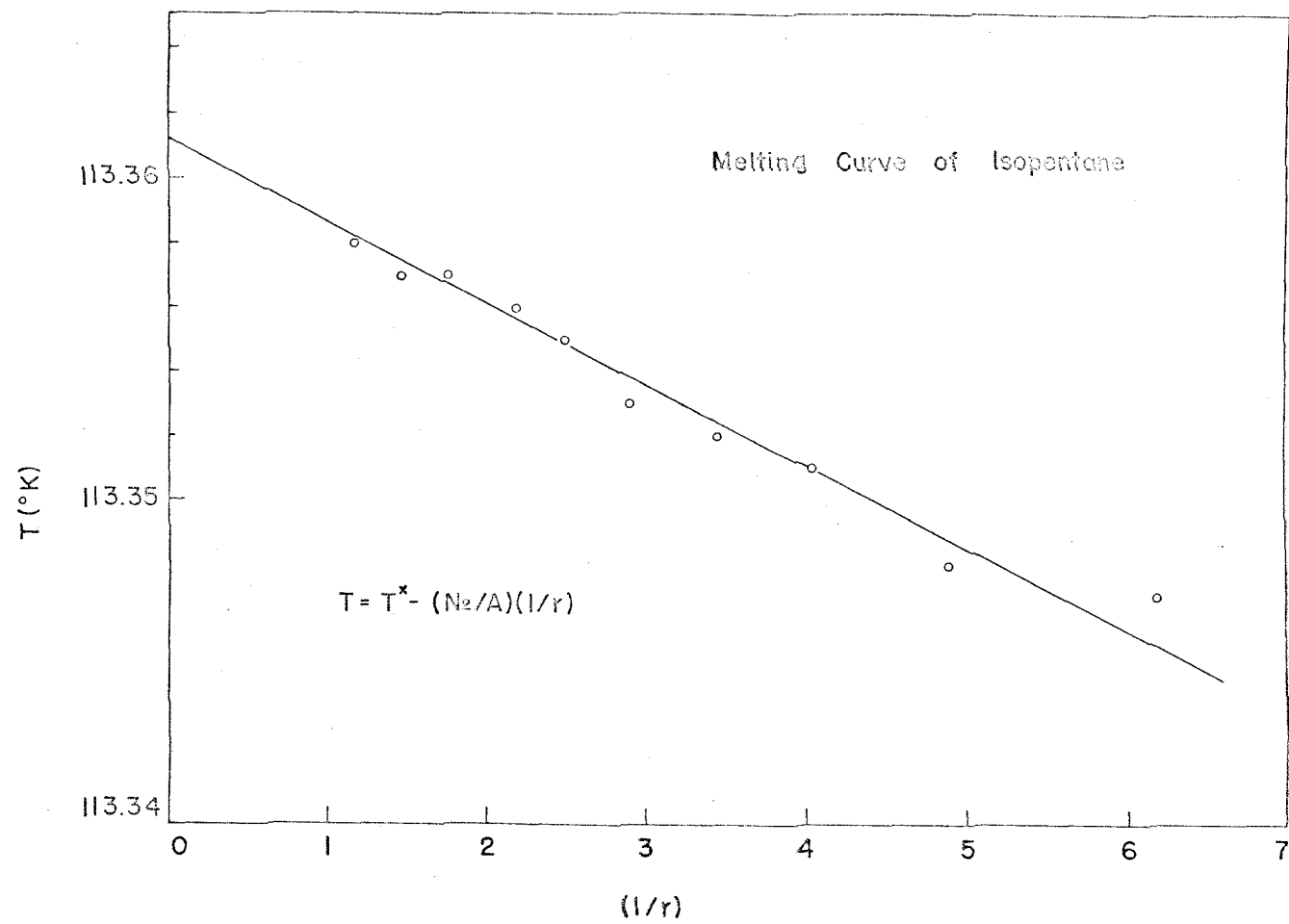


Fig. 5. Melting Curve of Isopentane.

amount of impurities in the present sample was found to be 0.014 mole per cent.

(b) Heat capacities of its glassy and supercooled liquid states. The numerical data are given in Table 4B and illustrated by the filled circles in Fig. 4. There appears a sharp rise of heat capacity at about 65°K, the shape of which is characteristic to a glass transition phenomenon. The amount of heat capacity of the supercooled liquid just above the glass transition point is nearly equal to the twice of that for the crystalline state and well situates on the assumed curve extrapolated from those above the melting point. When the supercooled liquid which had experienced the glass transition, was heated up to above the glass transition point, the drastic devitrification was found to take place at about 75°K. The results of the detailed measurements around  $T_g$  on the sample with the various heat treatments are shown in Fig. 6 and the enthalpy curves corresponding to each of them are drawn in Fig. 7. In the case of quenched sample, the enthalpy value of the supercooled liquid deviates from the equilibrium curve at about 66.5°K, and transforms into the glassy state. For slowly cooled sample, the curve deviates from the equilibrium value

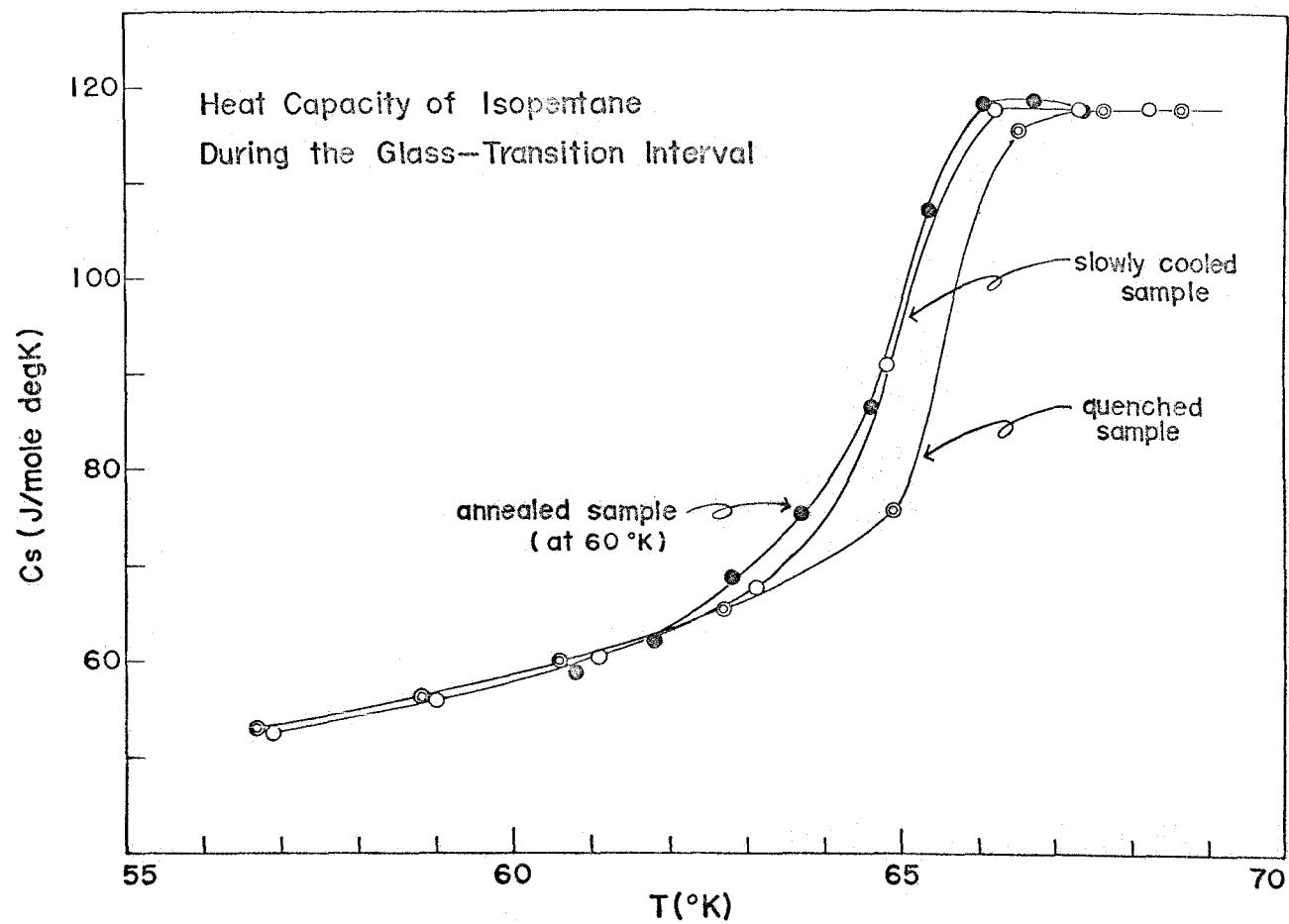


Fig. 6. Heat Capacity Curve of Isopentane in the Region of the Glass Transition Temperature.

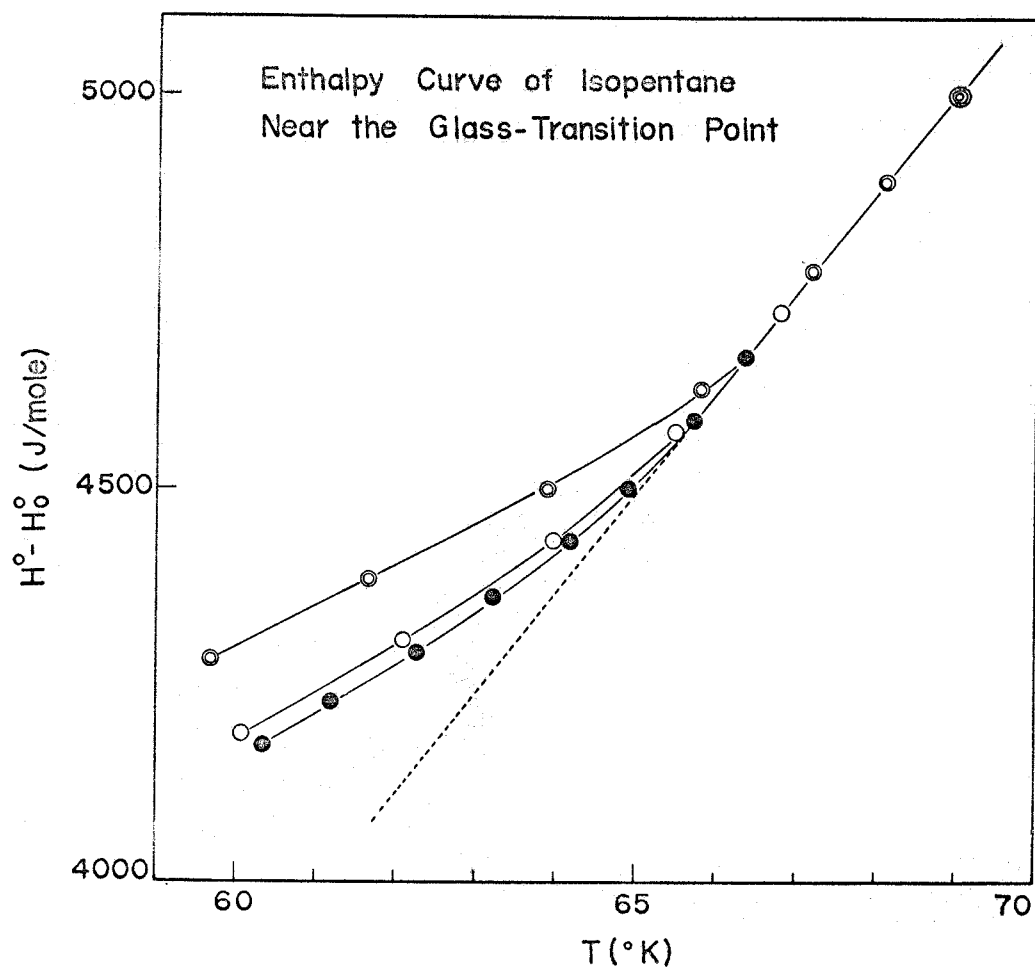


Fig. 7. Enthalpy Curve of Isopentane near the Glass Transition Point.

The double circles represent the quenched sample, the single circles the slowly cooled one, and the filled circles the annealed one. The triple circle : See text.

at the temperature  $1^{\circ}\text{C}$  lower than that for the quenched sample. The effect of annealing is really found in the enthalpy curve in such a way that the enthalpy curve of glass comes below the slowly cooled one. The triple circle near  $69^{\circ}\text{K}$  which is taken as the reference point for evaluation of absolute enthalpy of the glass, was determined as the intersection of the curve for supercooled liquid and the isenthalpy straight line at  $106.2^{\circ}\text{K}$  of the enthalpy curve for crystalline state.

3.2.2. Methanol. (a) Heat capacities of its crystalline state. The numerical data for the sample (2) are given in Table 6A, and are represented by the hollow circles in Fig. 8. In this figure the smoothed curve above  $120^{\circ}\text{K}$  is drawn on the basis of Kelley's data<sup>(28)</sup>. It is found that our present data below  $120^{\circ}\text{K}$  agree with his data within the experimental error of 1.3 % in the temperature region of liquid hydrogen, and 0.5 % in the temperature region of liquid nitrogen.

(b) Heat capacities of its glass and supercooled liquid states. The results of the samples (1) and (2) are given in Table 6B and illustrated by the filled circles in Fig. 8. In this figure, the values for

the sample (1) are plotted around the glass transition point and those for the sample (2) are plotted below 80°K (see Table 6B). As is seen in this figure it is found that the state of aggregation of methanol obtained by the present method of vapor condensation shows a glass transition phenomenon at about 103°K. On further heating we found a drastic devitrification phenomenon at about 105°K just above this glass transition point. The dotted line represents the assumed one for the supercooled liquid which are obtained by an extrapolation of those of the normal liquid. The jump of heat capacity ( $\Delta C_p$ ) at glass transition point ( $T_g$ ) and the total amount of exothermic effect accompanying the devitrification are given in Table 2. By comparing the heat of devitrification and the magnitude of  $\Delta C_p$  at  $T_g$  for both samples, it is easily concluded that the sample (1) is almost completely glassy state while the sample (2) is in the partially glassy state. In the Table 2 the amorphous part contained in the samples are also estimated by comparing the heat of devitrification with each other by assuming that the sample (1) is composed of 100 per cent amorphous material.

Table 6A. Heat Capacity of Methanol (crystal)  
in J/(mol °K).

T(°K)	Cs	T(°K)	Cs	T(°K)	Cs
21.61	6.019	51.28	23.94	84.40	38.24
23.97	7.402	55.26	25.75	88.47	40.07
26.66	9.311	58.74	28.25	92.46	41.49
29.73	11.30	62.46	29.98	96.30	42.33
32.93	13.29	65.91	31.69	100.25	43.21
36.25	15.57	69.68	32.82	104.29	44.51
39.83	17.59	73.73	34.44	108.22	45.76
43.51	19.87	77.56	36.39	112.04	46.83
47.24	21.84	79.92	36.64		

Table 6B. Heat Capacity of Methanol (glass and  
supercooled liquid) in J/(mol °K).

T(°K)	Cs	T(°K)	Cs	T(°K)	Cs
sample (1)		sample (2)			
series 1		series 1		series 4	
96.30	44.30	23.64	8.074	72.26	34.56
97.96	45.96	26.64	10.03	76.22	35.96
99.58	49.77	30.03	12.33	80.86	37.71
101.13	83.56			85.50	39.54
series 2		series 2		89.27	41.04
82.88	39.54	49.39	24.21	92.02	41.80
85.80	40.82	51.85	25.42	93.79	42.45
88.64	41.85	54.38	26.40	95.54	43.09
91.42	42.23	57.14	27.58	97.25	43.97
93.63	43.18	60.19	29.06	98.94	44.88
95.34	43.75	63.38	30.54	100.58	48.64
97.02	45.09	66.65	31.97	102.14	58.56
98.74	47.21	70.05	33.31	103.54	53.43
100.39	57.28	series 3		104.82	54.04
101.97	76.84	21.92	7.046	106.22	53.61
102.96	71.62	24.73	8.665		
103.87	68.92	27.86	10.79		
105.16	67.70	31.36	13.23		
		34.81	15.99		
		38.50	17.98		
		42.28	20.12		
		46.32	22.66		

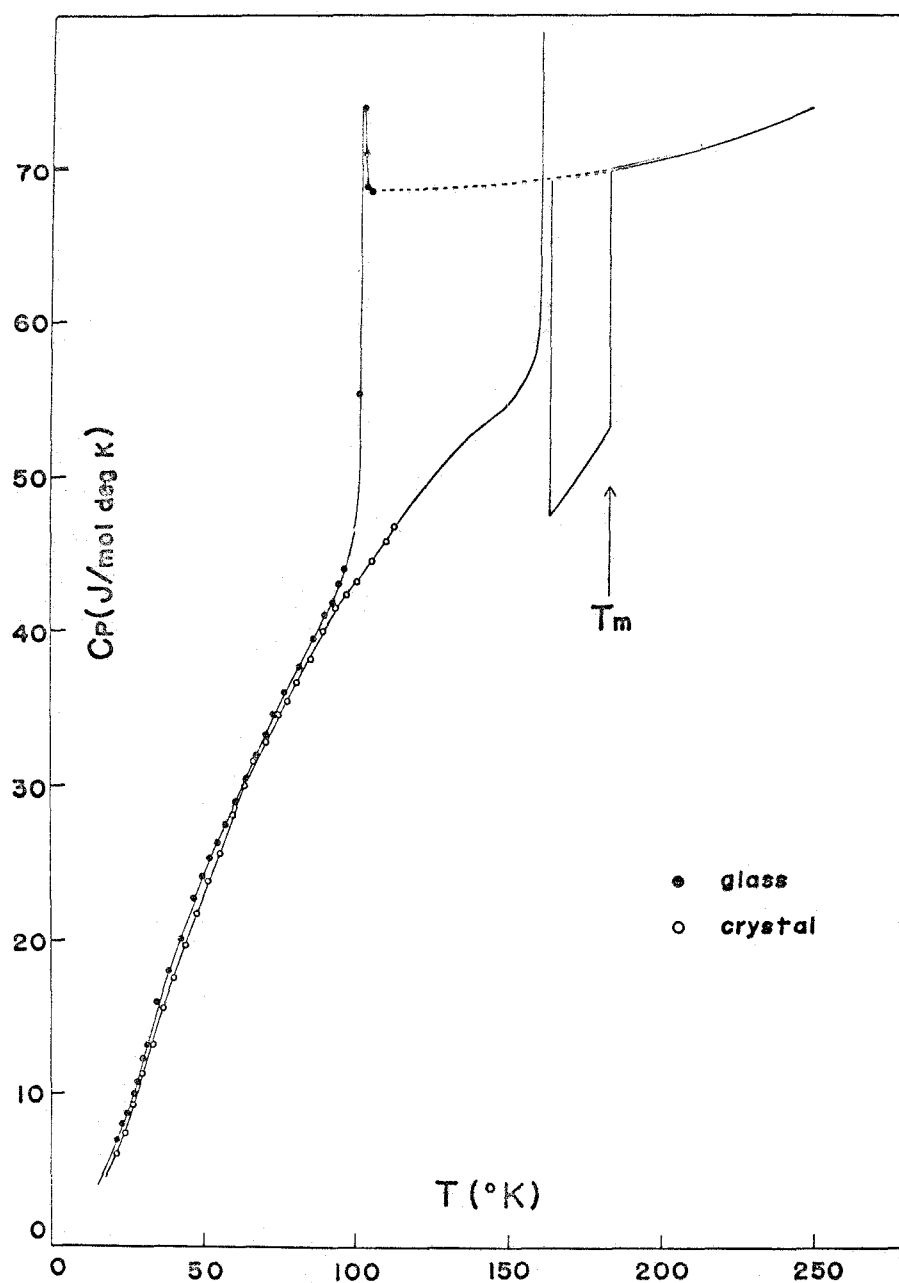


Fig. 8. Heat Capacity Curve of Methanol.



3.2.3. Water. (a) Heat capacities of hexagonal ice. The results of the samples (3) and (4) are given in Table 7A and are represented by the hollow circles in Fig. 9.

The values of our present data were smaller than those of Giaque's data<sup>(29)</sup> by 10 % because of the difficulty of estimation of the accurate weight of the sample in the calorimeter. This seems to be due to the fact that the some amount of water are condensed in the filling tube out of the sample cell and so the mole factor of the sample in the cell was estimated to be smaller than the true value. In this respect, the mole factors of the samples were determined by fitting our values of hexagonal ice to those of Giaque's data between 100° and 140°K. The deviation of the values around the smoothed curve is within 3 % in the vicinity of the boiling point of liquid nitrogen and 1 % around 200°K.

(b) Heat capacities of its glassy and supercooled liquid states. The results of the samples (1), (2), (3) and (4) are all given in Table 7B. The detailed values in the vicinity of the glass transition point are drawn in Fig. 10. The values of the sample (1) are plotted around  $T_g$  and those of the sample (3) below

80°K amongst all filled circles given in Fig. 9. As is seen in these figures the amorphous solid of water obtained by the method of vapor condensation was found to show a glass transition phenomenon at about 135°K. On further heating the drastic devitrification was found to occur just above the glass transition point. The jump of heat capacity at  $T_g$  and the total amount of exothermic effect accompanying the devitrification are given in Table 3, and the assumed content of the amorphous part of the samples are also given on the assumption that the sample (1) is composed of 100 per cent amorphous material.

(c) Heat capacities of cubic ice. The results of the samples (2), (3) and (4) are given in Table 7C, and are illustrated in Figs. 11 and 12 in comparison with the results of the hexagonal ice. As is seen in these figures, the remarkably anomalous region of heat capacities was found between 190° and 210°K, which is accompanied with an appreciable exothermic effect. Taking into consideration of the previous workers by the X-ray analysis which have reported that in this temperature region the cubic ice transforms sluggishly and irreversibly into the hexagonal ice, this exothermic effect seems to be due to the irreversible transformation

of this kind. The total exothermic effect was observed including the anomalous effect mentioned above in the wider temperature region from 160° to 210°K. The corresponding enthalpy amount of this exothermic effect was estimated for each specimen as is given in Table 8.

### 3.3. Thermodynamic Properties and Residual Entropy.

The values of heat capacity, entropy, and also the enthalpy and Gibbs energy functions at selected temperatures are listed for the liquid, crystalline, glassy, and supercooled liquid states of isopentane in Tables 9A and 9B, for the glassy state of methanol in Table 10.

The residual entropies,  $S_0^0$ , were also determined for isopentane and methanol by using the results of heat capacity measurements and given in Table 9B and 10. In the case of methanol we calculated the residual entropy on the basis of Kelley's data<sup>(28)</sup> for the crystalline state.

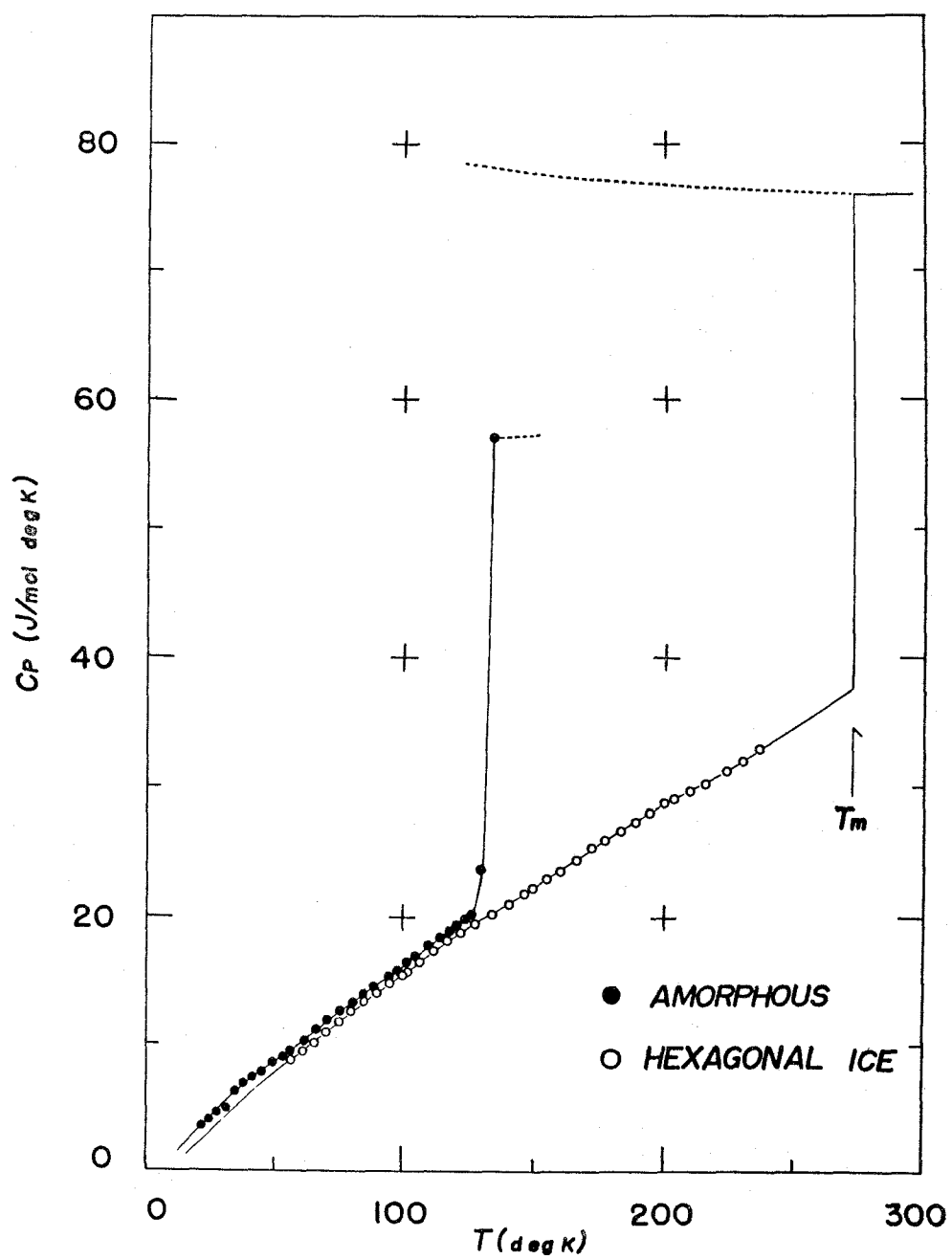


Fig. 9. Heat Capacity Curve of Water.

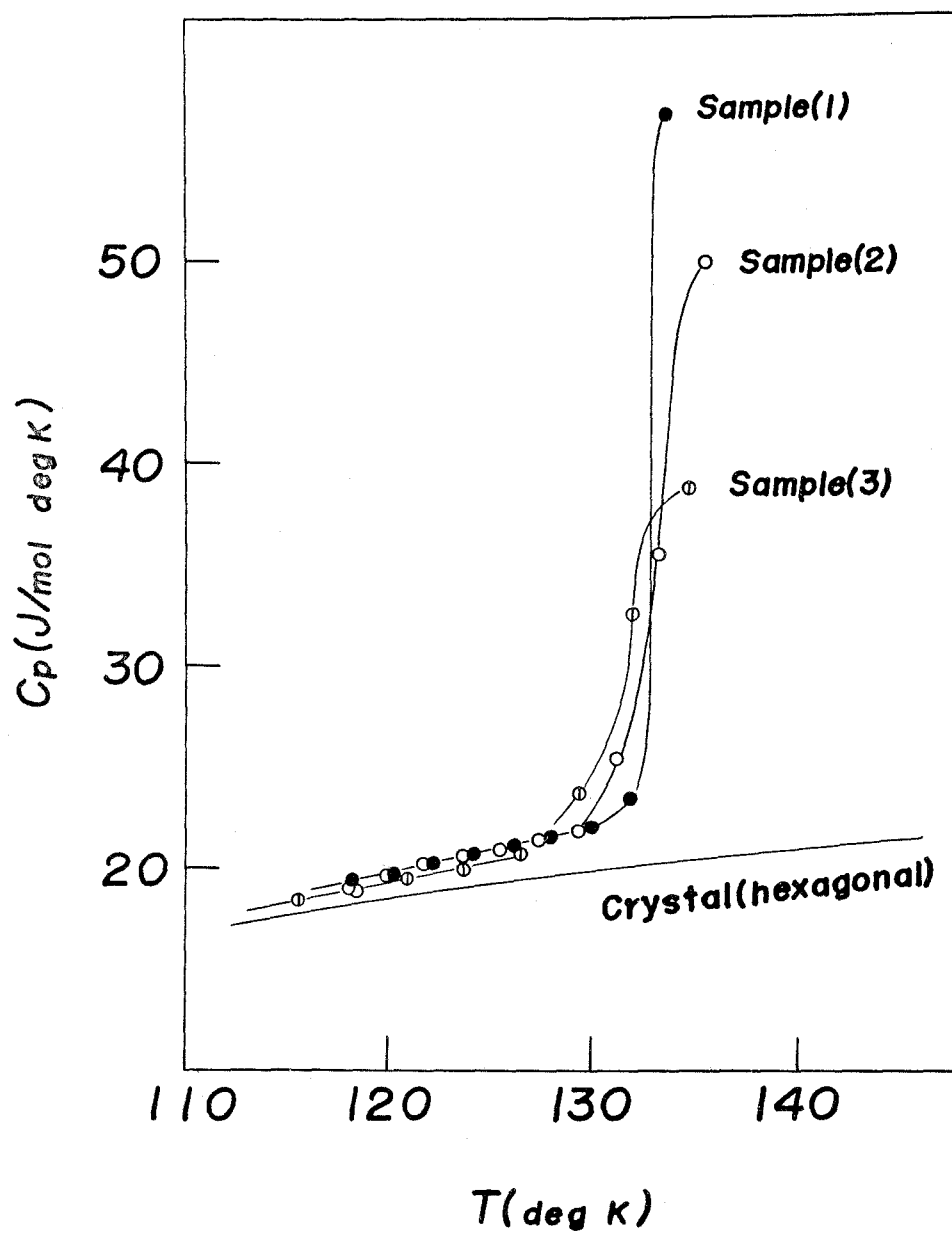


Fig. 10. Heat Capacity Curve of Water near the Glass Transition Temperature.

Table 7A. Heat Capacity of Water  
(hexagonal ice) in J/(mol°K).

T (°K)	Cs	T (°K)	Cs
sample (3)		sample (4)	
56.02	9.058	59.29	9.473
61.13	9.761	63.46	10.13
65.69	10.49	68.05	10.50
70.28	11.30	72.68	11.27
75.20	12.05	77.25	12.37
80.01	12.73	82.30	12.77
85.00	13.98	87.60	14.50
89.70	14.64	92.72	14.62
95.15	15.28	97.58	14.95
99.90	15.98	97.79	14.97
102.10	15.83	102.55	15.55
107.22	16.53	107.36	16.44
112.17	17.41	112.24	17.45
117.20	18.22	116.98	17.99
122.32	18.77	121.57	19.02
127.95	19.52	126.06	19.32
134.04	20.28	130.67	19.74
140.00	20.98	135.42	20.58
145.81	21.87	140.06	21.47
149.26	22.18	144.67	21.45
154.93	23.04	136.89	20.86
160.48	23.61	141.56	21.21
165.93	24.39	146.15	21.94
171.54	25.35	150.66	22.20
177.27	25.95	155.09	22.36
182.97	26.63	159.67	23.48
188.58	27.31	165.44	23.81
194.10	28.11	170.73	24.93
199.53	29.54	175.37	25.71
203.78	29.02	181.01	26.29
210.18	30.46	186.57	26.88
216.49	30.59	192.04	28.07
		197.44	28.82
		202.77	29.45
		208.03	30.20
		213.09	30.85

Table 7B. Heat Capacity of Water (glass and supercooled liquid) in J/(mol°K).

T(°K)	Cs	T(°K)	Cs	T(°K)	Cs
sample (1)		sample (3)		sample (4)	
118.82	19.42	21.75	3.644	79.98	13.71
120.21	19.63	24.73	3.957	84.23	14.29
122.23	20.17	27.75	4.061	88.51	14.78
124.21	20.64	31.10	4.685	92.93	15.27
126.17	21.12	34.53	6.378	97.50	15.88
128.11	21.45	38.10	7.002	101.91	16.63
130.01	21.89	41.70	7.393	106.49	17.19
131.88	23.37	45.40	7.653	111.25	18.17
133.58	57.30	49.33	8.590	115.88	19.09
135.86	46.47	53.56	9.032	120.38	19.88
		57.83	9.501		
sample (2)		58.04	9.527	series after annealing at 128°K for 12 hours	
		62.22	10.26		
		66.59	11.24		
118.05	19.20	71.24	11.92	119.95	19.30
119.90	19.72	76.05	12.68	122.16	19.93
121.81	20.21	80.80	13.30	124.35	20.33
123.72	20.49	85.27	14.47	126.52	21.17
125.61	20.83	89.74	14.86	128.69	22.31
127.48	21.38	94.23	15.28	130.90	24.49
129.35	21.78	98.57	15.75	132.73	28.14
131.23	25.44	102.75	16.50	134.18	31.51
133.19	35.42	104.94	16.97		
135.50	50.04	109.77	17.67		
		114.46	18.35		
		118.20	18.90		
		121.01	19.39		
		123.79	19.94		
		126.56	20.72		
		129.34	23.74		
		131.97	32.36		
		134.67	38.47		

Table 7C. Heat Capacity of Water  
(cubic ice) in J/(mol°K).

T (°K)	Cs	T (°K)	Cs	T (°K)	Cs
sample (2)		109.94	17.36	sample (4)	
		114.64	18.27		
182.56	24.73	119.20	19.13	60.14	9.496
187.11	25.71	123.69	19.65	64.62	10.41
191.64	25.80	128.33	20.20	69.14	11.02
196.19	24.05	133.07	20.85	73.72	12.12
200.59	27.40	137.70	21.55	78.21	12.35
204.87	29.25	142.28	22.18	82.68	13.15
209.08	30.04	146.77	22.65	87.47	13.94
213.26	30.07	151.18	23.48	92.56	14.34
217.39	30.44	155.79	23.64	97.44	14.95
221.48	31.19	159.67	23.01	97.72	14.95
		164.57	23.69	102.76	15.58
sample (3)		170.40	24.18	107.77	16.51
		176.11	25.25	112.61	17.47
21.62	1.275	181.79	26.32	117.32	18.22
24.08	3.019	187.47	26.94	121.90	18.85
26.64	3.462	193.15	25.25	126.10	19.48
29.79	4.139	198.82	26.60	126.62	19.74
33.45	5.076	204.24	29.13	130.92	20.02
37.24	5.805	210.08	30.12	131.43	20.00
41.00	6.716	216.36	30.85	135.64	20.84
44.83	7.106	222.55	31.81	136.17	20.98
48.82	8.069			140.26	21.40
53.10	8.434			144.82	22.29
57.63	8.980			149.30	22.62
58.98	9.397			153.72	22.97
63.25	10.26			156.21	23.53
67.54	11.04			162.22	23.32
72.10	11.66			168.17	24.04
76.86	12.21			174.03	24.40
81.57	13.38			179.82	25.03
86.02	14.03			185.51	26.10
90.51	14.58			191.14	26.80
95.08	15.16			196.77	25.57
99.49	15.54			202.24	28.91
103.75	16.16			208.07	29.77
108.11	17.02			214.34	30.83
				220.52	31.34



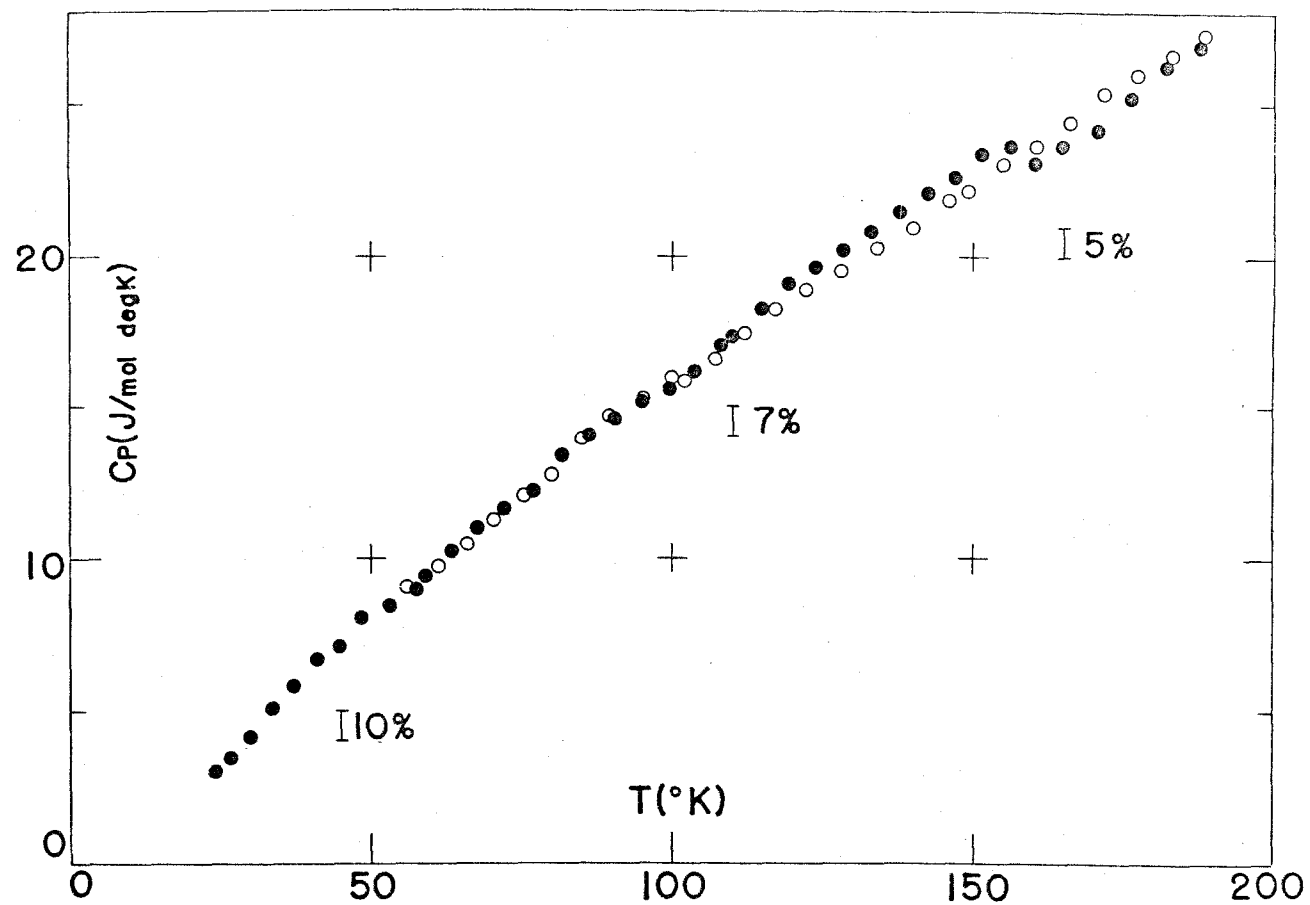


Fig. 11. Heat Capacity of Ice.  
 The filled circle represents the cubic ice and the hollow circle the hexagonal one.

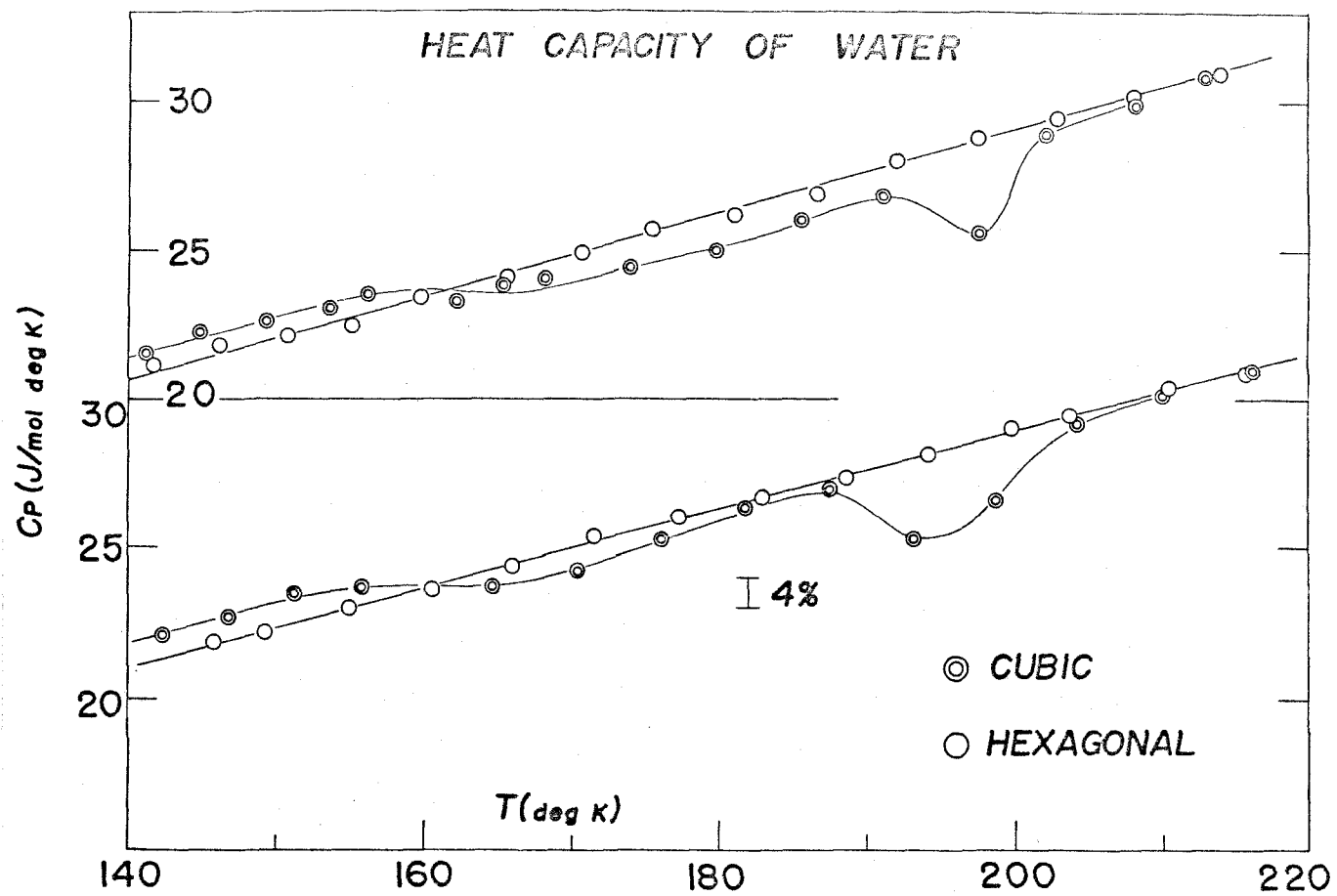


Fig. 12. Heat Capacity of Ice near the Transformation Temperature.

(Cubic  $\rightarrow$  Hexagonal)

Table 8. Total Amount of Exothermic Effect  
Accompanying Irreversible Transformation of  
Cubic Ice to Hexagonal Ice.

Number of sample	$-\Delta H$ (J/mol)	
2	158.9	} $\pm 15$
3	164.4	
4	159.5	

Table 9A. Thermodynamic Properties of Isopentane  
(crystalline and liquid states)  
in J/(mol degK).

T	$C_p^O$	$S^O$	$(H^O - H_0^O)/T$	$-(G^O - H_0^O)/T$
5	(0.255)	(0.085)	(0.063)	(0.021)
10	(2.030)	(0.655)	(0.499)	(0.155)
15	6.430	2.236	1.667	0.569
20	12.47	4.893	3.596	1.297
30	24.76	12.32	8.642	3.678
40	35.21	20.93	14.03	6.903
50	43.60	29.71	19.12	10.59
60	51.92	38.38	23.88	14.50
70	63.08	47.12	28.59	18.53
80	63.88	55.43	32.79	22.64
90	71.25	63.38	36.65	26.72
100	78.72	71.27	40.48	30.78
110	86.81	79.14	44.32	34.82
113.36	Fusion			
120	124.42	134.19	92.78	41.41
140	127.74	153.59	97.51	56.08
160	130.97	170.87	99.01	71.86
180	134.38	186.48	104.96	81.52
200	138.17	200.83	100.08	92.74
220	142.50	214.20	110.01	104.19
240	147.63	226.81	113.84	112.97
260	153.60	238.85	116.66	112.19
280	159.62	250.46	119.52	130.94
300	166.82	261.70	122.42	139.28

Values in parentheses are extrapolated by means of the Debye function.

Table 9B. Thermodynamic Properties of Isopentane  
(glassy and supercooled liquid states)  
in J/(mol degK).

T	$C_P^O$	$S^O - S_0^O(\text{gl})^*$	$(H^O - H_0^O(\text{gl}))/T$	$-(G^O - H_0^O(\text{gl}))/T$
5	(0.365)	(0.122)	(0.091)	(14.09)
10	(2.880)	(0.977)	(0.735)	(14.30)
15	8.660	2.951	2.373	14.64
20	15.03	6.315	4.733	15.65
30	26.95	14.73	10.21	18.58
40	36.75	23.88	15.67	22.27
50	45.13	32.97	20.72	26.31
60	58.77	42.16	25.70	30.52
70	117.28	55.45	38.60	30.91
80	118.63	71.21	48.52	36.75
90	119.98	85.26	56.38	42.94
100	121.33	97.72	62.81	48.97
110	122.67	108.68	68.19	54.55

$$S_0^O(\text{gl}) = 14.06 \text{ J/(mol degK)}; H_0^O(\text{gl}) - H_0^O(\text{c})^{**} = 2673 \text{ J/mol.}$$

The values between 70° and 110°K are evaluated by means  
of interpolation using equation  $C_P = 107.82 +$   
 $0.1351T$  (J/mol degK).

\*: (gl) indicates glassy state.

\*\* : (c) indicates crystalline state.

Table 10. Thermodynamic Properties of Methanol  
(glassy and supercooled liquid states)  
in J/(mol°K).

T(°K)	$C_P^O$	$S^O - S_0^O(\text{gl})^*$	$(H^O - H_0^O(\text{gl}))/T$	$-(G^O - H_0^O(\text{gl}))/T$
5	(0.310)	(0.082)	(0.070)	(0.012)
10	(1.700)	(0.619)	(0.447)	(0.172)
15	(4.350)	(1.796)	(1.297)	(0.499)
20	7.250	3.444	2.421	1.023
30	13.75	7.572	5.081	2.491
40	19.96	12.40	8.043	4.357
50	25.30	17.44	10.97	6.466
60	30.02	22.48	13.76	8.720
70	34.42	27.44	16.40	11.04
80	38.59	32.31	18.91	13.40
90	42.40	37.07	21.31	15.76
103	Glass transition point			
110	68.10	48.65	28.04	20.61
120	68.39	54.59	31.38	23.21
130	68.70	60.05	34.24	25.81
140	68.98	65.16	36.71	28.45
150	69.20	69.90	38.87	31.03
160	69.41	74.39	39.78	34.61
175.22	70.00	80.70	43.27	37.43

$$S_0^O(\text{gl}) = 7.07 \text{ J/(mol°K)}; H_0^O(\text{gl}) - H_0^O(\text{c})^{**} = 1538 \text{ J/(mol)}.$$

The values in parentheses are extrapolated by means of the Debye function.

\* : (gl) indicates glassy state.

\*\* : (c) indicates crystalline state.

#### [4] DISCUSSION

##### 4.1. Glass Transition and Devitrification Phenomena.

4.1.1. Isopentane. The heat capacities of isopentane have been measured by three investigators<sup>(26, 27, 30)</sup>, nevertheless the occurrence of the glassy state of this compound had not been known by any authors. It must be noted here that a supercooled liquid of isopentane are often called as a glass in error<sup>(31)</sup>. As is already remarked in the introductory chapter of the thesis, a modern terminology for "glass" must not be used for the supercooled liquid state above a glass transition point. We have really succeeded in obtaining the glassy state of the present material. The relation of the normal boiling point to its normal melting point of isopentane is equal to 2.70. This fact is concordant with the Turnbull-Cohen empirical rule<sup>(32)</sup> for obtaining glassy state by the supercooling method; i.e. the ratio should be equal to or larger than 1.8. In passing we may describe here our experience on n-pentane. The ratio  $T_b/T_m = 2.15$  for this substance suggests that this liquid might have also the tendency to be supercooled,

whereas the crystallization has always occurred as far as our observation is concerned.

Now, for liquid isopentane two kinds of origin associated with the relaxation phenomenon in regard to the molecular motion may be possible to consider; one is due to the degree of freedom of the internal rotation with respect to the intramolecular C-C bond, and the other due to the change of the intermolecular configuration which is related to the shear and/or volume viscosity of liquid isopentane. Concerning the liquid state of isopentane, there is an investigation with an ultrasonic absorption technique by Young and Petrauskas<sup>(33)</sup>. Their results suggest that around 150°K the relaxation time with respect to the degree of freedom of internal rotation is larger than that for intermolecular configurational change. It is not clear, however, how is the relation between these two types of relaxation time for the supercooled liquid around 65°K. We may safely conclude, anyhow, that  $\Delta C_p$ , the increment of heat capacity at the glass transition point, is mainly associated with intermolecular configurational change, since the difference between the contributions from the intramolecular rotation in the supercooled liquid and that in the



glass, may be too small to explain this  $\Delta C_p$ .

4.1.2. Methanol. Van Thiel and Pimentel<sup>(7)</sup> observed that methanol deposited on the chilled substrate between 4.2° and 120°K gives an infra-red absorption spectrum resembling that of the normal liquid methanol, and that once this deposited state was heated up above 120°K, the spectrum disappeared and changes to that characteristic of the crystalline state. Based on the above observation, they have conjectured that this deposited state of methanol might be a glass. However, their conclusion seems too hasty, because a glass transition phenomenon, which necessarily accompanies the glassy state, has not been yet found out. Therefore our present finding of the glass transition phenomenon certifies for the first time that the methanol condensed onto the chilled substrate below 105°K exists as a glassy state. Moreover, it is to be noted that the vitreous methanol of the sample (1) is composed of about 100 per cent amorphous material judging from the heat of devitrification as well as the jump height of heat capacity,  $\Delta C_p$ , at  $T_g$ .

In general, it seems very difficult to obtain

the completely vitreous state by the method of vapor condensation. In fact there has been no quantitative work of obtaining completely vitreous material by this method. In case of our calorimetry, the temperatures of several parts of the apparatus can be regulated accurately and finely and also the rate of condensation can be controlled very precisely during the vitrification process, so that it is rather easy to obtain a completely vitreous material, when the suitable condition for the adjustment of temperature distribution is established. The fact that the sample (2) contains the appreciable crystalline part seems to be due to the warming up of the surface of the sample above the devitrification point by the high rate of condensation.

4.1.3. Water. (a) Glass transition phenomenon. Since Jones and Simon<sup>(34)</sup> first tried to find out a glass transition phenomenon of water by a rapid cooling of droplet of the order of few microns, there have been several trials to discover the glass transition phenomenon of an amorphous state deposited on a chilled substrate. They are, for example, of Pryde and Jones (1952)<sup>(16)</sup>, of Ghormley (1956)<sup>(18)</sup>, of de Nordwall and Staveley (1956)<sup>(19)</sup>, and of McMillan and Los (1965)<sup>(11)</sup>

Recently, McMillan and Los have found by a

differential thermal analysis method an endothermic effect at 139°K just below a devitrification temperature, their experiment was, however, insufficient to conclude that this endothermic effect might be due to a glass transition phenomenon. In the present work we have found out the anomalous heat capacity for four species characteristic of the glass transition phenomena at about 135°K. Judging from the shape of the anomalous heat capacity, and from its temperature dependence on annealing treatment, it seems evident that this effect is due to the so-called glass transition phenomenon.

Although the exothermic effect observed below  $T_g$  is shortly understood as an approach of the glassy state to an equilibrium (the so-called stabilization effect), we conclude that this exothermic effect is also partly due to a devitrification of the glassy state. This is evidenced by the fact that the exothermic effect was observed even after the annealing at 128°K for 16 hours, and that the heat of devitrification is smaller as the duration of annealing is longer (see Table 3), and further that the heat capacity curves of two series do not agree with each other in the case of the sample (4), as is shown in Fig. 13, where one series of measurements is made prior to annealing and the other after annealing at 128°K for 13 hours.

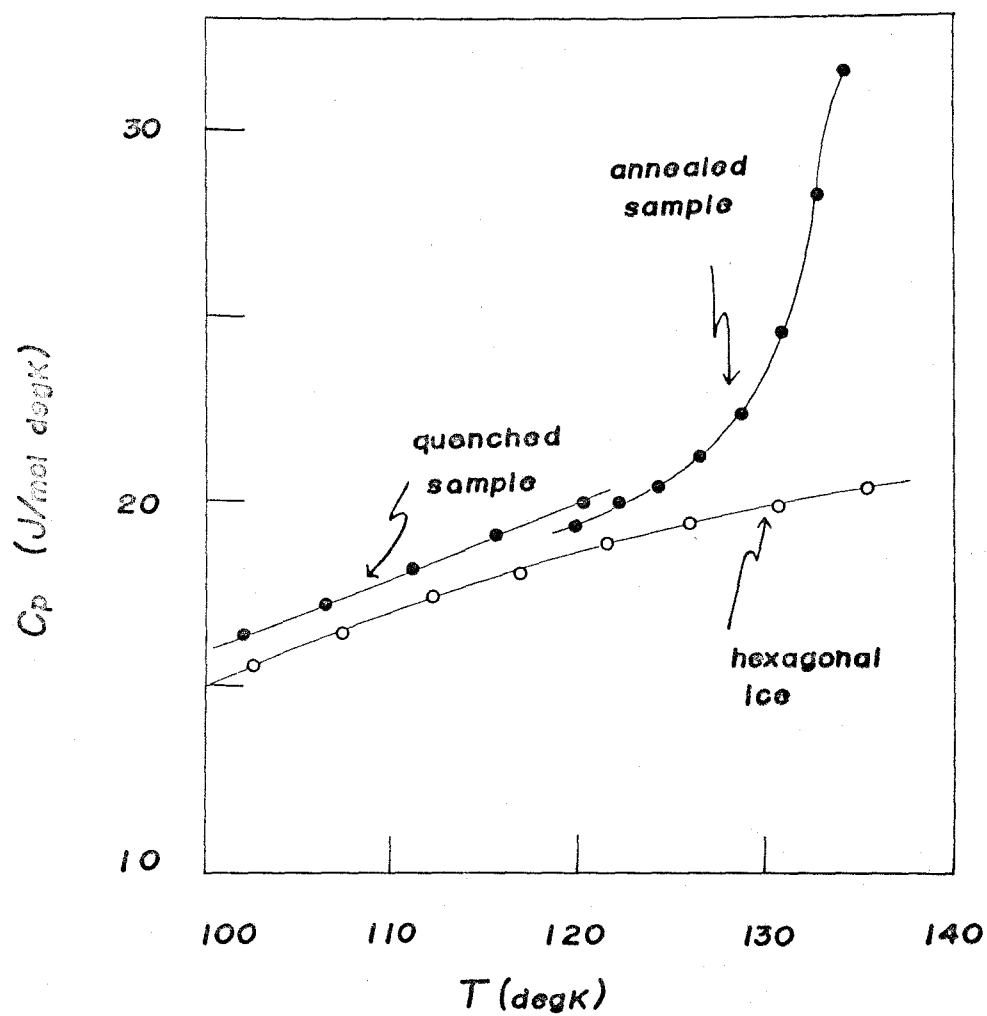


Fig. 13. Heat Capacity of the Glassy State of Water.

In the case of sample (1), the jump height of heat capacity  $\Delta C_p$  at  $T_g$  is the highest value among all samples (see Table 3 and Fig. 10). The heat capacity just above the  $T_g$  of this sample, however, appreciably smaller than that of the supercooled liquid at the same temperature assumed by the extrapolation of the heat capacity of the liquid above the melting point. This fact is at the first glance considered to be due to the existence of crystalline part in the vitreous sample. This interpretation seems, however, to be inadequate because of some thermodynamical contradiction as will be described just below. If  $C_p$  values of the supercooled liquid are assumed to be extended like a dotted line in Fig. 9, the corresponding enthalpy curve of the supercooled liquid comes out to be drawn in Fig. 14. At first sight of this figure it is shortly understood that the curve of the supercooled liquid intersects that of the crystal far above 135°K ( $=T_g$ ). This circumstance is evidently incompatible with the fact that the devitrification is necessarily accompanied by the exothermic effect. Consequently, it turns out to be inappropriate to assume the  $C_p$  values of the supercooled liquid by extrapolating the  $C_p$  values of the liquid above the melting point down to the lower temperature.

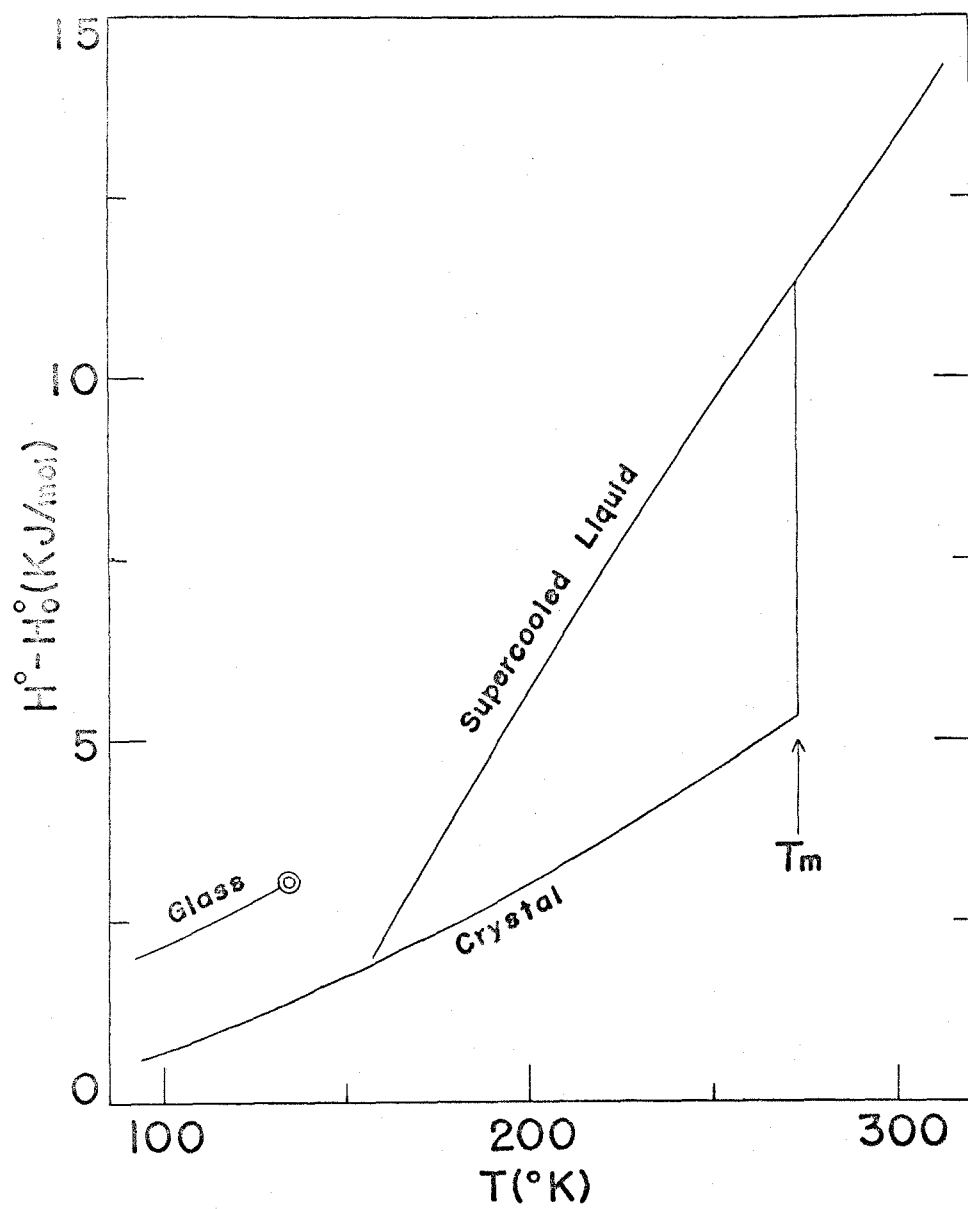


Fig. 14. Enthalpy Relationship of Various States of Water.

Now, water has been known as a typical anomalous liquid, for example, its  $C_p$  values are higher than those of other normal liquids. In order to interpret the remarkably abnormal physical properties, Eucken<sup>(35)</sup> has proposed that water is an equilibrating mixture of several kinds of associated species (e.g.,  $H_2O$ ,  $(H_2O)_2$ ,  $(H_2O)_4$  and  $(H_2O)_8$ ), and that the anomalous large value of heat capacity is caused by dissociation of the associated species with the rise of the temperature. Recently, Wada<sup>(36)</sup> has calculated the heat capacity of water reduced to a normal liquid assuming the existence of two states in water such as icy and packed states. According to his calculation, the  $C_p$  value of water reduced to the normal liquid is smaller than that of crystal at  $0^\circ C$ . Therefore his calculation does not directly stand for our present results. However, this plausible interpretation that the intrinsic  $C_p$  value of water consisting of exclusively monomer molecules might be smaller than the really observed one, seems undoubtedly to support that the vitreous water obtained in the present work (in particular sample (1)), may be in the nearly 100 per cent amorphous state.

(b) Devitrification phenomenon. The temperature region and the heat of devitrification have been reported

by many workers. Their data are compared with each others in Table 11.

In the experiments by de Nordwall and Staveley<sup>(19)</sup> by Ghormley<sup>(18)</sup> and by us, it was found that the process of the devitrification proceeds in two steps. The explanation of the reason why such a stepwise phenomenon appeared is not clear at the present state of investigation.

Here we may notice again that all the data except ours are got by the thermal analysis method, hence the previous data are to some extent for the non-equilibrium state.

(c) Appearance of the cubic ice and its transformation into the hexagonal ice. During past many years, a great deal of investigations have been reported concerning the appearance of the cubic ice and its transformation to the hexagonal ice (see Table 1). As the results of these studies it is now well known that the cubic form of ice can be obtained either as a product of devitrification of amorphous ice or as a kind of high pressure form. In this section, we should like to concern only with the cubic ice prepared by the former method.

Up to the present, the existence of sluggish and



Table 11. Comparison of Previous Data  
for Heat of Devitrification.

Workers	- $H_D$ (cal/g)	Temperature region
Pryde and Jones <sup>(16)</sup>	2~7	144°K
de Nordwall and Staveley <sup>(19)</sup>	3~10	140°~160°K
Ghormley <sup>(18)</sup>	15.8	153°~198°K
Beaumont et al. <sup>(24)</sup>	12	140°~156°K
Ghormley <sup>(38)</sup>	24±2	153°~193°K
Present work	21.8	135°K

irreversible transformation of the cubic ice to the hexagonal ice has been observed by several workers. There has been no quantitative experiments on the sample in the thermodynamically equilibrium state, so there remain still a confusion about the temperature interval of the appearance of the cubic ice, and also a more important problem whether the cubic ice is more stable than the hexagonal ice or not in the lower temperature region as is already pointed out in the introductory chapter.

According to our present heat capacity measurements, the cubic ice transforms sluggishly and irreversibly into the hexagonal ice with an appreciable exothermic effect between 160° and 210°K. The average total amounts of the exothermic enthalpy change, 160 J/mol, is close to the value, 150 J/mol, previously reported by McMillan and Los. This agreement however, seems to be fortuitous, because their experiment is of dynamical nature and their results are based on the Ghormley's value<sup>(18)</sup> (1.26 KJ/mol) for the heat of devitrification which does not agree with our present data (1.64 KJ/mol)

As is well known, the hexagonal ice has a center of symmetry in the direction vertical to c-axis and a mirror of symmetry in the direction parallel to this axis with regard to the conformation of oxygen atoms

in the lattice. On the other hand the cubic ice has the center of symmetry in these two directions, i.e., a diamond structure. Each unit of the both conformations of the oxygen atoms is illustrated in Fig. 15A. The total structures composed of these units are shown in Fig. 15B in the cases of the cubic and hexagonal ices.

The enthalpy change of the transformation amounting to about 160 J/mol, which is obtained in the present experiment, is considered to be due to the difference of the lattice energy between both structures. Such an exothermic phenomenon seems to be concordant with the result calculated by Bjerrum<sup>(37)</sup>, i.e., the hexagonal ice is more stable than the cubic ice with regard to its lattice energy.

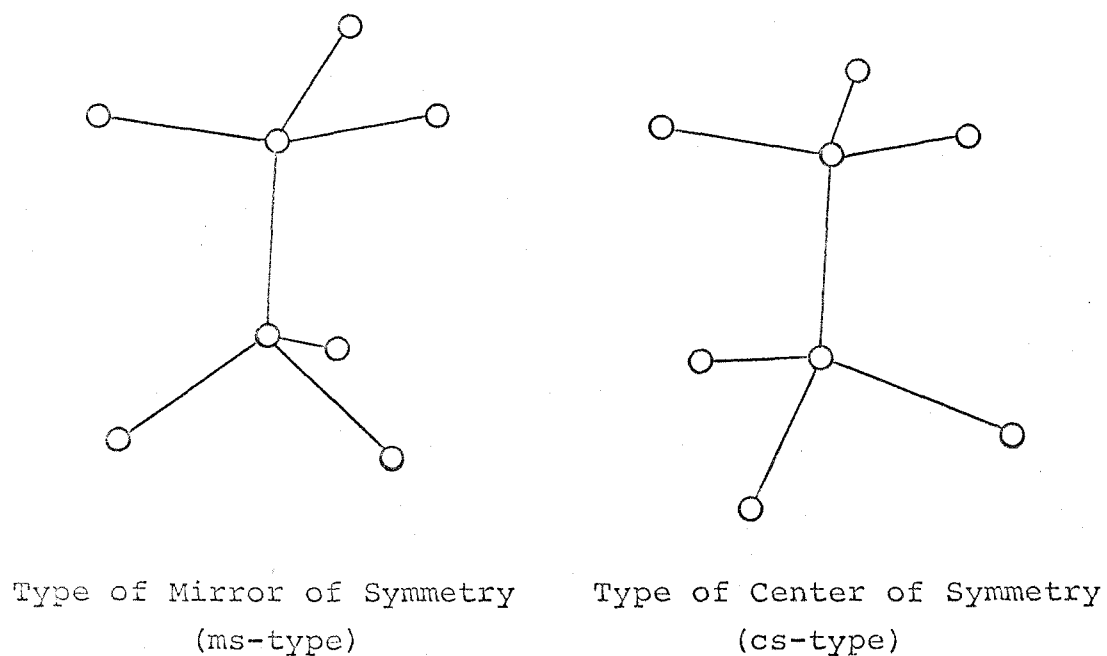


Fig. 15A. Units of Conformation of Oxygen Atoms.

The spheres stand for the oxygen atoms, the solid lines the hydrogen bonds.

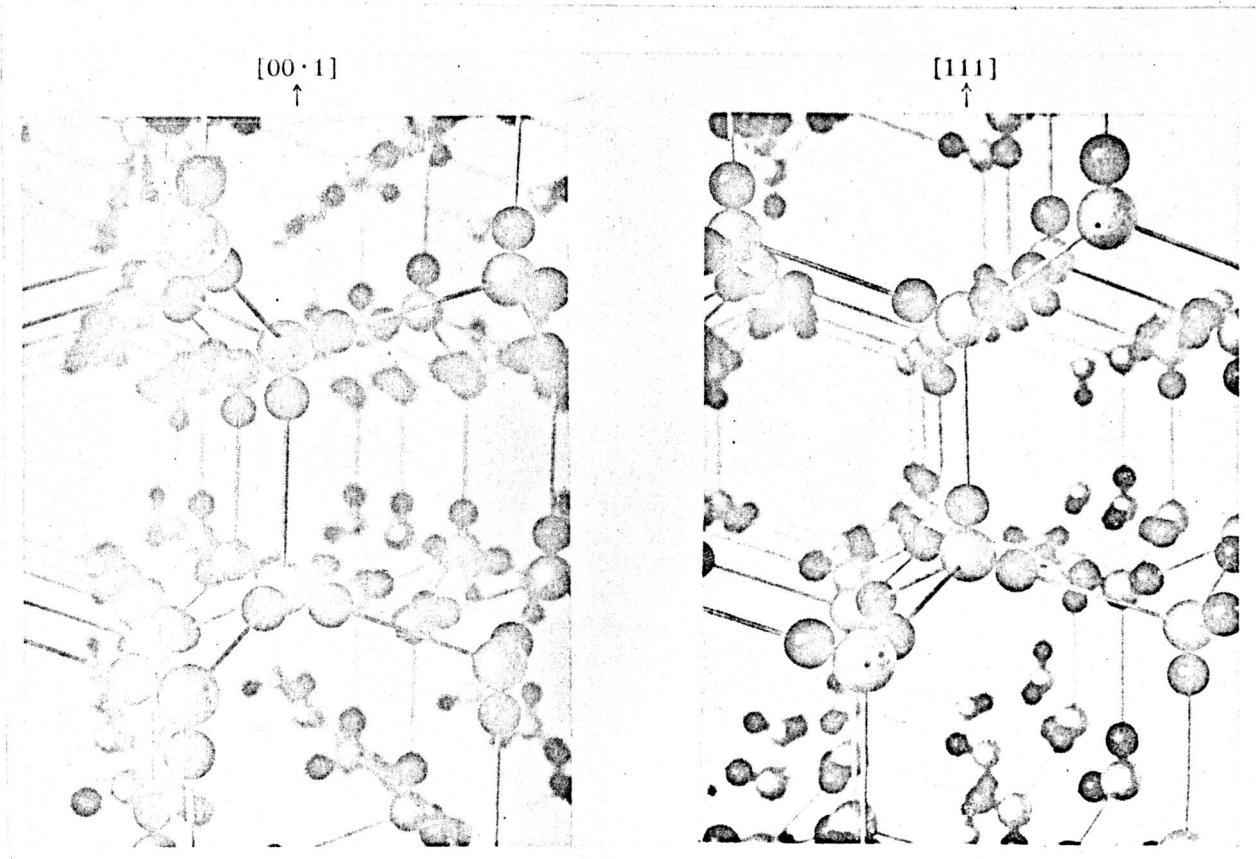


Fig. 15B. Models of the Crystal Structures of Ice.

(from H.Gränicher, Z. Krist. 110,432(1958)

The left photograph represents the hexagonal ice viewed vertically to the c-axis, the right one the cubic ice viewed vertically to the [111]-axis. The white sphere indicates the oxygen, the black one the hydrogen atoms, in no relative dimensions. As the atomic radius of oxygen amounts to 1.38 Å and O-H distance 0.99 Å, the hydrogen atoms in real crystal may be embedded in the electron clouds of the oxygen atoms.

#### 4.2. Origin of Glass Transition Phenomenon.

It is widely known that the glass transition temperature  $T_g$ , where the various properties of the supercooled liquid and/or of the glass change suddenly, is found out to be evidently dependent upon the magnitude of duration of the experimental observation. This fact undoubtedly suggests that the glass transition phenomenon originates from a certain kind of rate processes. As a matter of fact, there has been proposed many successful kinetic theories to explain the observation of the frequency-dependent properties around the glass transition point. On the other hand there exists also the thermodynamical interpretation of this phenomenon. It is to be noted here that the past theories explaining the really observed glass transition phenomenon as a second-order phase transition in the sense of the Ehrenfest's classification is now quite nonsense. Because the really obtained glassy state does not in an equilibrium state at all. We never designate here such a mistaken view as the thermodynamical theories.

In his famous paper<sup>(40)</sup> Kauzmann has pointed out the fact that there seems to appear the thermodynamically unthinkable circumstances if we could perform the experiment during the infinitely long period. For example,

we follow his statement using the entropy curve of isopentane which was obtained by the heat capacity measurement.

If we could chill the supercooled liquid at an infinitely low rate, the glass transition phenomenon never occurs and its entropy curve might be such as drawn by a broken line in Fig. 16 where it is represented as an ideally supercooled liquid. At first sight of this figure, it is shortly understood that the curve of this ideally supercooled liquid intersects that of the crystalline state at a unique temperature. Below this temperature the entropy values of the supercooled liquid are rather smaller than those of crystal. This circumstance seems to be unthinkable because a liquid state is generally considered to be of a more appreciably disordered state than the crystalline one. This thermodynamically unusual situation is well known as a Kauzmann's paradox. And the temperature where the entropy curve of the supercooled liquid intersects that of the crystal, was first called at  $T_2$  by Gibbs et al<sup>(41)</sup>.

What is meant by this peculiar way of thinking? Adam and Gibbs have thought that there might exist a certain kind of thermodynamically definable phase transition at  $T_2$ , and that in the vicinity of this

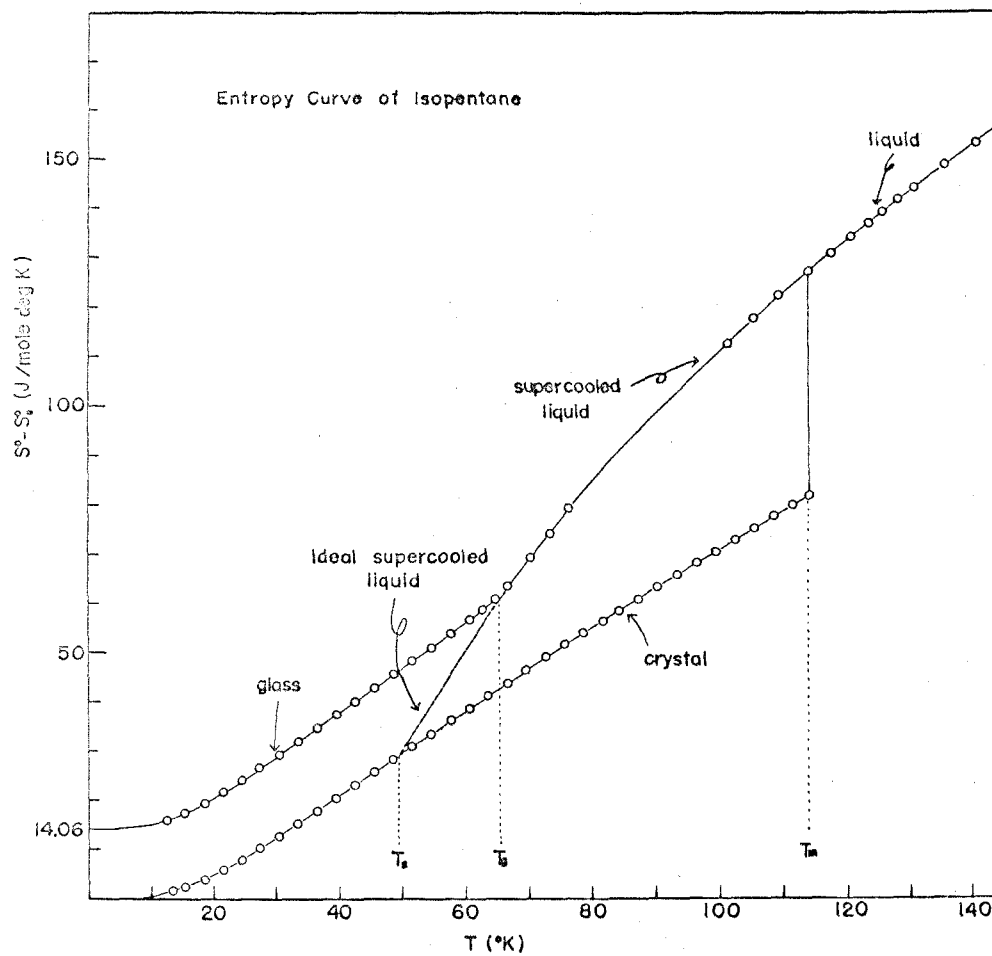


Fig. 16. Entropy Curve of Isopentane.



temperature  $T_2$ , the proper relaxation time of the system has a tendency to attain quite a large value. As a result the system really goes into a glassy state even when it is chilled down as slowly as possible, because our present available duration of the experiment has an inevitable upper limit.

By explaining the appearance of the glass transition in such a way as mentioned above, Adam and Gibbs are trying to grasp the glass transition as a reflection of the thermodynamically definable phase transition. It is to be noted here that the experimentally observed glass transition is never definable by the usual thermodynamics and that their interpretation is very meaningful and suggestive for deeper consideration about the relation between an equilibrium and a non-equilibrium states.

In their suggestive paper, Adam and Gibbs have proposed that the temperature dependence of the relaxation time of liquid system, which characterize its response to an external force, might be given by the equation,

$$\tau(T) = A \exp(\Delta\mu s_C^* / TS_C) = A \exp(C/TS_C) \quad (4-2-1)$$

here  $A$  is the frequency factor and may not be dependent

upon temperature,  $\Delta\mu$  the potential energy barrier for the cooperative molecular rearrangement,  $S_C^*$  the critical configurational entropy of the representative cooperatively rearranging region with the lowest size, and  $S_C(T)$  the configurational entropy of the glass-forming liquid and can be calculated by using the difference of the heat capacity,  $\Delta C_p$ , between the glass-forming liquid and the glass, that is,

$$S_C(T) - S_C(T_2) = \Delta C_p \ln(T/T_2) . \quad (4-2-2)$$

If we use the assumption  $S_C(T_2)=0$ , which is explained in the preceding section, the above equation becomes

$$S_C(T) = \Delta C_p \ln(T/T_2) . \quad (4-2-3)$$

Furthermore, if we neglect the difference in the vibrational entropy between the hypothetical glass and the crystal at  $T_2$ , the residual entropy, i.e., the apparent entropy difference between glass and crystal at  $T=0^\circ\text{K}$  should be equal to the configurational entropy of the liquid which is "frozen in" at  $T_g$ .

Then, we have the next equation,

$$\Delta S_0 = ( S_{\text{glass}} - S_{\text{crystal}} )_{T=0} = S_C(T_g) . \quad (4-2-4)$$

Using equation (4-2-3) we get

$$\Delta S_0 = \Delta C_p \ln(T_g/T_2) . \quad (4-2-5)$$

Thus, from the results of heat capacity measurement the residual entropy  $\Delta S_0$  can be easily obtained, and then  $T_g/T_2$  is also estimated. This value  $T_g/T_2$  has been estimated by some previous workers, and they have found that the ratio,  $T_g/T_2$ , for many materials have a tendency to be 1.3.

By the way, we have 1.30 and 1.31 for isopentane and methanol, respectively. As is expected, our present values for methanol and isopentane are close to the reported value 1.3. This agreement seems to mean that Adam and Gibbs's theory might catch the essential features of the glass transition phenomenon.

#### 4.3. Appearance of Glass Transition Phenomenon as a Temperature Dispersion.

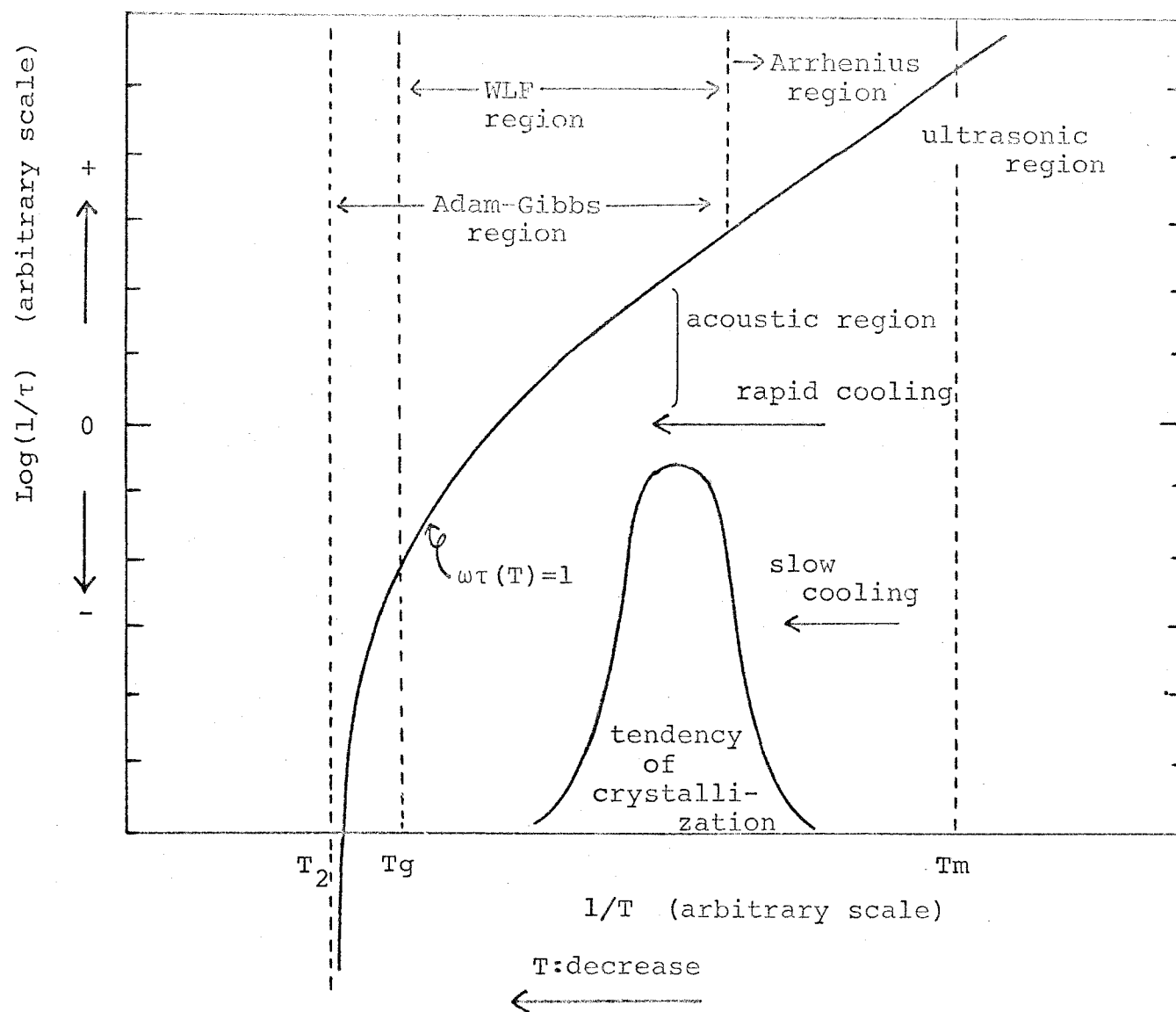
The term of "dispersion" generally means the fact that the quantity of a given physical property is dependent upon the duration of observation. In particular it is called an anomalous dispersion when the value of the relevant physical property changes

abruptly with a rather narrow frequency region. This anomalous dispersion effect originates from the fact that a relaxation time of the system, characterizing its response to an external force, becomes of the same order of magnitude with the duration of the observation. And the dispersion effect is called as a "frequency dispersion" when the frequency of an external force is changed and as a "temperature dispersion" when the temperature of the system is a variable.

After all, the frequency and the temperature take the same effect on the dispersion effect and this fact is called as "time-temperature equivalence". The observation with high frequency region is quite equivalent to the observation in low temperature region, and vice versa.

Now, the appearance of the glass transition phenomenon does indisputably originate from this anomalous dispersion effect. These circumstances are conceptually depicted in Fig.17. The values of  $\tau(T)$  is a relaxation time characteristic of the system, and dependent on the temperature. This curve is sorted out in three temperature regions, i.e., one is that where the Arrhenius equation is available, second where WLF empirical rule holds good and third where the Adam and Gibbs theory is available. The anomalous dispersion effect can be

Fig. 17. Temperature Dependence of the Relaxation Time.



observed on the curve of the equation  $\omega\tau(T)=1$ . Within the temperature region below this curve, the system behaves as a glass, and in the upper temperature region it behaves as a liquid. On such a viewpoint, therefore, there are possible to exist infinitely many glass transition temperatures which are defined in a wider sense than usual.

Next, we should like to sketch the temperature dispersion effect of the liquid system considering the rather simplified model of the liquid in the temperature region where the Adam-Gibbs theory is available.

As is usually adopted, we assume that the physical properties of the liquid materials can be separated into the two parts, that is, one is due to the degree of freedom characteristic exclusively of a liquid, and the another is due to the degree of freedom characteristic of a glass. Then, for example, the heat capacity of the actual liquid system,  $C_{liq}$ , can be represented as follows,

$$C_{liq} = C_{gl} + C_{str} \quad (4-3-1)$$

where  $C_{gl}$  is the heat capacity of the glass and  $C_{str}$  the heat capacity characteristic exclusively of the liquid. Next, let's suppose that the liquid as a

whole consists of two subsystems of "structural" and "glassy" which are connected with a hypothetical tube whose thermal conductivity is represented by  $\kappa(T)$ , as is drawn in Fig. 18.

If this liquid system is brought to be thermal contact with an external cold reservoir, how does this system respond to this thermal disturbance? This causes the system to lose some amount of enthalpy at a constant rate,  $-\dot{\Delta H}_{liq}$ , which is supplied by the "structural" and "glass" systems, so that the following relation holds,

$$\dot{\Delta H}_{liq} = \dot{\Delta H}_{gl} + \dot{\Delta H}_{str} \quad (4-3-2)$$

As the both subsystems lose their enthalpies with the passage of time, their temperature decreases. Here  $\dot{\Delta H}_{gl}$  is not dependent upon the temperature and  $\dot{\Delta H}_{str}$  is necessarily dependent upon the both temperatures  $T_{gl}$  and  $T_{str}$  in the vicinity of  $T_g$ .

Assuming further the following relations

$$\left. \begin{aligned} \dot{\Delta H}_{str} &= \kappa (T_{str} - T_{gl}) \\ \kappa &\propto 1/T \end{aligned} \right\} \quad (4-3-3)$$

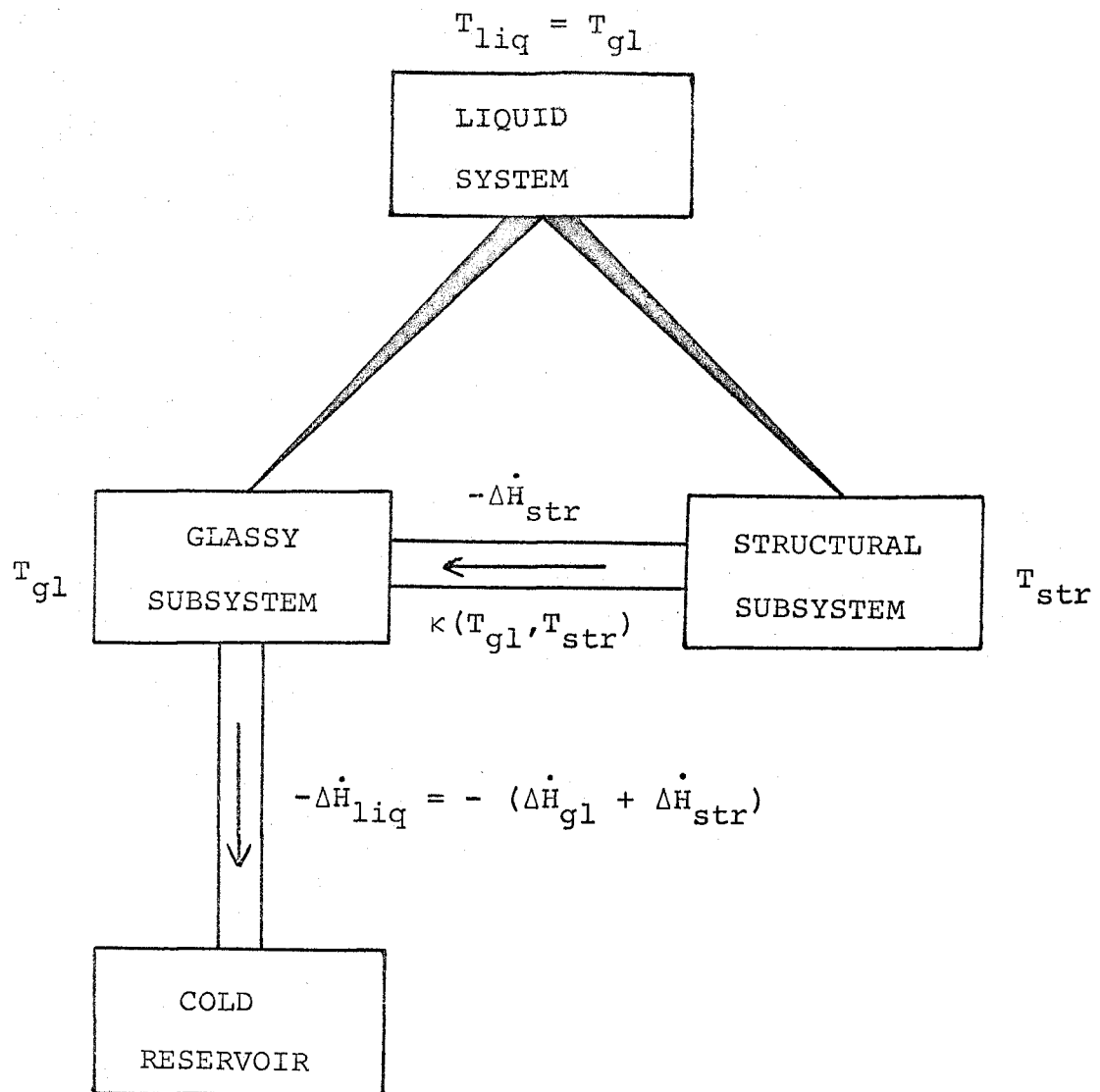


Fig. 18. Sketch of the Typification of the Hypothetical Heat Flow in a Liquid.



and following the theory of Adam and Gibbs (see equation 4-2-1), we have

$$\tau(T) = 1/\kappa = A \exp(C/TS_C) \quad (4-3-5)$$

in the vicinity of the temperature  $T_2$  as was described already.

Consequently, when the temperature of the system, which is identical to the temperature of the "glass" subsystem, approaches this temperature  $T_2$ , the relaxation time  $\tau$  tends to become very large. This causes  $\dot{\Delta H}_{str}$  to be a very small value. Really, if the value of  $\tau$  becomes to be the same order of magnitude with the duration of experiment, the liquid system tends to deviate from its inner thermal equilibrium. And finally,  $\Delta H_{str}$  becomes zero when the value of  $\tau$  becomes of the order much larger than the duration of the actual experiment.

In that case the heat capacity of the liquid system is given by

$$\begin{aligned} C_{liq} &= (\dot{\Delta H}_{gl} + \dot{\Delta H}_{str}) / \dot{\Delta T}_{gl} = \dot{\Delta H}_{gl} / \dot{\Delta T}_{gl} \\ &= C_{gl} < (C_{gl} + C_{str}) \end{aligned} \quad (4-3-6)$$

Consequently, the heat capacity of the liquid really decreases abruptly at a certain temperature. This is concordant with the really observable behavior of heat capacity. The temperature, where the sudden change occurs, is naturally the glass transition temperature which is usually observed above  $T_2$  by about  $50^\circ\text{C}$ . In this respect the appearance of the glass transition may be thought as an example of the temperature dispersion effect.

After all, we can expect that the glass transition phenomenon must be observed for every materials if we can use an appropriate method and suitable condition. The vapor condensation method adopted in the present investigation will promise a fruitful future study on some simple molecular glasses.

#### 4.4. Entropy Production and Residual Entropy.

A few comments will be given here concerning the relation between the residual entropy and the entropy production of the irreversible phenomenon taking part in a glassy state.

Just below the glass transition temperature, we can observe usually an exothermic effect due to the

stabilization phenomenon of the glassy state into a supercooled liquid.

This stabilization gives rise to an irreversible entropy production within the system. It is well known that the residual entropy of the glassy state generally involves the excess entropy due to this irreversible phenomenon. Davies and Jones<sup>(42)</sup> suggested the possibility that this entropy production can be estimated by considering the heat conduction between subsystems of "structural" and of "glassy", each of which is in different temperatures in the glassy state.

Consequently, the irreversible production of entropy,  $\Delta S_{irr}$ , can be expressed very simply by the following expression

$$\Delta S_{irr} = \Delta C_p (1/\bar{T} - 1/T) \Delta T, \quad (4-4-1)$$

where  $\Delta C_p$  is the heat capacity of structural part,  $T$  the temperature of a glass, and  $\bar{T}$  the fictive temperature of a structural system.

In order to estimate this quantity, the drift of temperature of the sample, for example, of isopentane was measured for long time during the glass transition intervals. This drift corresponds to the time derivative of  $T$ , and/or  $\bar{T}$ . Analyzing the results of the drift

curve for the quenched sample,  $\Delta\bar{T}$  was found to be  $-0.089^{\circ}\text{C}$  with the assumption that structural heat capacity is equal to that of the glass. Taking the following data  $\bar{T}=65^{\circ}\text{K}$ ,  $T=60^{\circ}\text{K}$ ,  $\Delta C_p=16.3 \text{ cal}/(\text{mol } ^{\circ}\text{K})$  we get  $\Delta S_{\text{irr}}=0.019 \text{ cal}/(\text{mol } ^{\circ}\text{K})$  which is very small compared with the residual entropy at absolute zero,  $S_0=3.36 \text{ cal}/(\text{mol } ^{\circ}\text{K})$ .

We can safely conclude that the neglect of the irreversible production of entropy leads to no significant error on determining the residual entropy.

#### 4.5. Definition of Glassy State.

In this section we do not want to give the detailed molecular description of a glassy state, but to discuss the characteristics which distinguish the glassy state from other states of aggregation.

A glassy state has been commonly considered as a non-crystalline solid obtained by supercooling of a liquid, when the glass transition phenomenon has been always observed. However, the non-crystalline solid can be also obtained by using other rather uncommon methods, such as vapor condensation, neutron bombardment, and others. This non-crystalline solid has

been observed to be crystallized on heating. For this kind of solid, the glass transition phenomenon has not ever been observed. As far as the glass transition phenomena are not observed, we may feel a certain hesitation to call this non-crystalline solid as a glass. However, our new findings of the glass transition phenomena of methanol and water produced by the vapor condensation method conclude that the non-crystalline solids of these materials made by this uncommon method must be called as a glass. On the basis of our new observation we may propose a more general property of the glassy state as follows.

- (a) First of all, the glassy state must be distinguished from other states only by the fact that the thermodynamically equilibrium state is never attained.
- (b) The glassy state must show the glass transition phenomenon which characterizes the boundary between the glassy and supercooled liquid states.
- (c) The glassy state is established irrespective of either the method of preparation or the chemical construction of the material.

Therefore, if we could not observe the glass transition phenomenon concerning the non-crystalline solid, we must be as careful as possible to call its

state as a glass, till its glass transition phenomenon is really found out.

[5] CONCLUSION

(1) The two types of calorimeter were constructed for the study of glass transition phenomena. One of them is for such a purpose that the vitrification is performed by a rapid cooling of a liquid sample in the calorimeter cell and the other is for the sample which is vitrified with condensation of its vapor directly on the chilled wall of the calorimeter cell.

(2) a) The heat capacity measurements were performed for the crystalline, liquid, glassy and supercooled liquid states of isopentane between 13° and 300°K by using the former calorimeter. b) The glass transition phenomenon of isopentane was found near 65°K with the drastic change of the heat capacity which amounts to 68.20 J/(mol °K). c) The residual entropy of the glassy isopentane at absolute zero was found to be 14.06 J/(mol °K). d) The irreversible entropy production of isopentane during the glass transition intervals was found to be 0.08 J/(mol°K). It is concluded that the neglect of the irreversible production of entropy leads no significant error in determining the residual entropy.

(3) a) The heat capacity measurements of methanol were

made for the crystalline state between 20° and 120°K, and for the glassy and supercooled liquid states between 20° and 105°K by using the latter type of the calorimeter. b) The glass transition phenomenon was found near 103°K with the abrupt change of the heat capacity which amounts to 26 J/(mol°K). c) The drastic devitrification with the exothermic effect which amounts to 1.54 KJ/mol was observed near 105°K. The residual entropy for the glassy methanol at absolute zero was found to be 7.07 J/(mol°K).

(4) a) In the case of water, the heat capacity measurements were carried out for the hexagonal crystal between 60° and 250°K, for the cubic crystal between 20° and 240°K, and for the glassy and supercooled liquid states between 20° and 136°K. b) The glass transition phenomenon was found near 135°K with the sudden change of the heat capacity amounting 35 J/(mol°K). c) The drastic devitrification with the exothermic effect which amounts to 1.64 KJ/mol was observed at about 135°K. d) The transformation of the cubic crystal to the hexagonal one was found to occur irreversibly and sluggishly in the temperature region from 160° to 210°K where the exothermic effect coming to about 160 J/mol was observed.



(5) The origin of the glass transition phenomenon was discussed and concluded that the appearance of the glass transition phenomenon is due to the anomalous dispersion effect, although this phenomenon is closely connected with some thermodynamical quantities in the equilibrium state.

(6) It was proposed that the non-crystalline solid deposited on the chilled substrate from the vapor state must show the glass transition phenomenon. This proposition was really confirmed by our experiments on methanol and water.

(7) Definition of the glassy state was proposed in such a way that it must be in the thermodynamically non-equilibrium state, and that it must show necessarily the glass transition phenomenon.

[6] BIBLIOGRAPHY

1. V. Regnault, Pogg. Ann. Physik, 98, 396(1856).
2. F. Simon, Ann. Physik, 68, 278(1922).
3. D. R. Secrist and J. D. Mackenzie,  
"Modern Aspect of the Vitreous State" edited by J. D.  
Mackenzie (Butter Worths Scientific Publication, Ltd.,  
London, 1964) volume 3, chapter 6.
4. M. Goldstein, J. Chem. Phys., 39, 3369(1963).
5. G. Adam and J. H. Gibbs, J. Chem. Phys., 43, 139(1965).
6. H. J. de Nordwall and L.A.K. Staveley,  
J. Chem. Soc., 1954, 2240.
7. G. C. Pimentel and A. L. McClellan,  
" The Hydrogen Bond " (W. H. Freeman and Company,  
San Francisco and London, 1960), p. 103 .
8. J. A. McMillan and S. C. Los,  
J. Chem. Phys., 42, 829(1965).
9. L. C. Shepley and A. B. Bestul,  
J. Chem. Phys., 39, 680(1963).
10. C. A. Angell, E.J. Sare, and R. D. Bressel,  
J. Phys. Chem., 71, 2759(1967).
11. J. A. McMillan and S. C. Los,  
Nature, 206, 806(1965).
12. E. F. Burton and W. F. Oliver,  
Proc. Roy. Soc., A153, 166(1935).

13. L. Staronka, Roczniki Chem., 19, 201(1939).
14. L. Vegard and S. Hillesund,  
Avh. norske Vidensk Akad., NO.8, 1(1942).
15. H. König, Nachr. Akad. Wiss. Göttingen, NO.1, 1(1942),  
Z. Krist. 105, 279(1943).
16. J. A. Pryde and G. O. Jones,  
Nature, 170, 685(1952).
17. G. Honjo and K. Shimaoka,  
Acta Cryst., 10, 710(1957).
18. J.A. Ghormley, J.Chem. Phys., 25, 599(1956).
19. H. J. de Nordwall and L. A. K. Staveley,  
Trans. Faraday Soc., 52, 1061(1956).
20. M. Blackman and N. D. Linsgarten, Proc. Roy. Soc.,  
A239, 93(1957). N. D. Linsgarten and M. Blackman,  
Nature, 178, 39(1956).
21. F. V. Shallcross and G. B. Carpenter,  
J. Chem. Phys. 26, 782(1957).
22. J. G. Dowell and A. P. Linfret,  
Nature, 188, 1144(1960).
23. K. Shimaoka, J. Phys. Soc. Japan, 15, 106(1960).
24. R. H. Beaumont, H. Chihara, and J. A. Morrison,  
J. Chem. Phys., 34, 1456(1961).
25. H. Suga and S. Seki,  
Bull. Chem. Soc. Japan, 38, 1000(1965).
26. G. B. Guthrie Jr. and H. M. Huffman,  
J. Am. Chem. Soc., 65, 1139(1943).

27. S. C. Schuman, J. G. Aston , and Malcolm Sagenkahn,  
J. Am. Chem. Soc., 64, 1039(1942).
28. K. K. Kelley,  
J. Am. Chem. Soc., 51, 180(1929).
29. W. F. Giaugue and J. W. Stout,  
J. Am. Chem. Soc., 58, 1144(1936).
30. G. S. Parks, H. M. Huffman and S. B. Thomas,  
J. Am. Chem. Soc., 52, 1032(1930).
31. O. Janseen and K. Funabashi,  
J. Chem. Phys., 46, 101(1967).
32. D. Turnbull and M. H. Cohen,  
J. Chem. Phys., 29, 1049(1958).
33. J. M. Young and A. A. Petrauskas,  
J. Chem. Phys., 25, 943(1956).
34. G. O. Jones and F. E. Simon,  
Endeavour, 8, 175(1949).
35. A. Eucken, Nachricht. Akad. Wiss. Göttingen,  
Math. Physik Klasse S. 38 (1946)
36. G. Wada, Bull. Chem. Soc. Japan, 34, 955(1961).
37. N. Bjerrum , Kgl Danskab. Selskab. Math-fys.  
Medd, 27, 1(1951): Science, 115, 385(1952).
38. J. A. Ghormley, J. Chem. Phys., 46, 1321(1967).
39. H. Gränicher, Z. Krist., 110, 432(1958).
40. W. Kauzmann, Chem. Rev. 43, 219(1948).

41. J. H. Gibbs, " Modern Aspects of the Vitreous State "  
edited by J. D. Mackenzie (Butter worths Scientific  
Publication, Ltd., London, 1960), volume 1, chapter 7.
42. R. O. Davies and D. O. Jones,  
Proc. Roy. Soc., A217, 26 (1953).